HOXB7 overexpression leads triple-negative breast cancer cells to a less aggressive phenotype

Simone Aparecida de Bessa Garcia
I3S: Universidade do Porto Instituto de Investigacao e Inovacao em Saude
Mafalda Araújo
I3S: Universidade do Porto Instituto de Investigacao e Inovacao em Saude
Tiago Pereira
I3S: Universidade do Porto Instituto de Investigacao e Inovacao em Saude
Renata Freitas (renata.freitas@ibmc.up.pt)
I3S: Universidade do Porto Instituto de Investigacao e Inovacao em Saude https://orcid.org/0000-0002-0123-7232

Research

Keywords: Breast Cancer, HOXB7, Invasion, Metastasis, MDA-MB-231

Posted Date: January 19th, 2021

DOI: https://doi.org/10.21203/rs.3.rs-147853/v1

Abstract

Background

Breast cancer is a serious public health issue worldwide and, despite the advances in the understanding of this disease, its great complexity and heterogeneity still represent a major hurdle for accurate diagnosis and therapy decision-making. In addition to the biomarkers found to be useful in the prognosis a treatment of breast cancer, *HOX* genes have been proposed to be involved in the progression of this disease. For example, *HOXB7* alterations in the expression and methylation patterns have been reported to promote breast cancer progression, most likely in a molecular subtype dependent way.

Methods

Here we induced *HOXB7* overexpression in MDA-MB-231 cells, cellular model of Triple-Negative Breast Cancer, and evaluated the phenotypic changes in cell viability, morphogenesis, migration, invasion and formation of colonies. We also evaluated the expression of putative downstream targets and their direct binding to HOXB7 by Chip-qPCR in *HOXB7*-overexpressing cells and controls, namely *CTNNB1*, *EGFR*, *FGF2*, *CDH1*, *DNMT3B* and *COMMD7*.

Result

During the phenotypic characterization of the *HOXB7*-overexpressing cells, we found consistently a less aggressive behavior represented by lower cell viability, inhibition of cell migration, invasion and attachment-independent colony formation capacities added to the more compact and organized spheroids growth in 3D culture. In addition, we detected that these phenotypic changes may relate to the direct or indirect interaction of the HOXB7 protein with *CTNNB1*, *EGFR*, *FGF2*, *CDH1*, *DNMT3B* and *COMMD7* genes.

Conclusion

Taken together, these results highlight the plasticity of the HOXB7 function in breast cancer, according to the cellular genetic background and expression levels and provide evidence that in triple-negative breast cancer cells, *HOXB7* overexpression has the potential to promote less aggressive phenotypes.

Background

Breast cancer is the most common cancer in women and a leading cause of cancer death among women worldwide [9]. In spite of the fact that a number of molecular biomarkers and gene signatures are being used in standard clinical practice, and a growing body of others are being studied and tested, the great complexity and heterogeneity of breast cancer still limits accurate diagnosis and therapy decision-

making [44]. In this context, HOX gene aberrant expression has been proposed as a breast cancer hallmark that is worth further investigation in order to improve prognosis and even develop novel targeted therapies [4, 10, 22]. The HOX genes are organized in four clusters in the human genome: HOXA (7p15), HOXB (17q21.2), HOXC (12q13) and HOXD (2q31). They are highly conserved from *Drosophila* to *Homo sapiens*, namely due to a characteristic feature: the homeobox sequence. This 180 base pair sequence encodes a terminal or sub-terminal tri-helical domain, the homeodomain [28, 40], which is responsible for the recognition and binding of the HOX proteins to specific DNA motifs (ATTA/TAAT) [12]. Apart from their role as transcription factors, the HOX proteins can also interact with other proteins to regulate cell or tissue-specific gene expression. Moreover, the genomic regions in which HOX genes are embedded produce numerous non-coding RNAs with important roles in gene regulation [23]. These “HOX products” have central roles during embryonic development [57] and are also required for maintenance of cellular homeostasis during adulthood [35].

In the breast, a structure that continues to form and remodel throughout a woman’s life, HOX genes assume a fundamental role in normal development and disease conditions [17], as their aberrant expression is frequently associated with breast tumorigenesis [22]. This is the case of *HOXB7*, a gene expressed during the branching of the ductal tree and alveolar bud differentiation and also during the involution process after lactation [22]. This HOX gene has a tendency to be overexpressed in primary breast cancer tumours with a more prominent overexpression in metastasis [67] and has also shown to be overexpressed in a variety of cell lines representative of distinct molecular subtypes [22, 27]. Among breast cancer cell lines representing four molecular subtypes, the highest *HOXB7* expression was detected in Luminal A and B models (MCF7 and BT474, respectively), and the lowest was observed in Triple Negative (MDA-MB-468 and MDA-MB-231) and HER2 + models (SKBR3) [27]. These subtype-specific expression profiles suggest that *HOXB7* may have distinct roles in different breast cancer contexts [22, 31].

In vivo and *in vitro* breast cancer models have associated the increased levels of *HOXB7* with the activation of TGFB signalling [47]) and with the expression levels of HER2 [33] and EGFR [32]. Studies performed in transgenic mice suggest that *HOXB7* promotes breast cancer progression and metastisation by activating the TGFB signalling pathway [47]. It was suggested that activation of TGFB/SMAD3 signaling is activated by HOXB7, because SMAD3 phosphorylation seems to be higher in primary mammary tumours from Hoxb7/Her2 double-transgenic mice than from Her2/neu single-transgenic mice. These authors also provide evidence that HOXB7 may bind to the *TGFB2* promoter in double-transgenic tumours, in which TGFB2 expression is frequently higher than in single-transgenic mice. Moreover, TGFB2 expression was found to be higher in two breast cancer cell lines transfected with *HOXB7* (SKBR3, MDA-MB-231) and the knockdown of *TGFB2* in MDA-MB-231 cells overexpressing *HOXB7* seems to inhibit lung metastasis in mice.

To further study the impact of *HOXB7* modulation on Triple Negative Breast Cancer (TNBC), having the MDA-MB-231 cells as cellular model, we generated *HOXB7*-overexpressing clones in order to analyse the associated phenotypic changes. TNBC is a group of tumours characterized by the absence of the ER

(Estrogen Receptor) / PR (Progesterone Receptor) / HER2 expression, which represents for up to 15% of the cases, and have the worse overall survival and breast cancer cause-specific survival time, in every stage and sub-stage, when compared to non-TNBC [41, 45]. This high aggressiveness is represented by early relapses, few and non-targeted treatment options, and low response durability [54, 66]. We found that in a *HOXB7*-overexpressing clone cell viability was lower, cell migration, invasion and colony formation in soft agar were inhibited and sphere formation in 3D cultures appeared more organized. In addition, we detected that in the MDA-MB-231 cell model, the HOXB7 protein interacts with the promoter regions of *CTNNB1*, *FGF2*, and *CDH1* genes as *HOXB7*-overexpressing cells show an increment in *CDH1* interaction and *EGFR*, *DNMT3B* and *COMMD7* appear as potential new targets.

Overall, our results suggest that particular levels of *HOXB7* overexpression can inhibit the aggressive behavior of TNBC cells possible through the direct or indirect regulation of *CTNNB1*, *FGF2*, *CDH1*, *EGFR*, *DNMT3B* and *COMMD7*. This adds important information to the current understanding of the *HOXB7*-dependent signalling pathways in TNBC cells for which the discovery of reliable predictive biomarkers is imperative for improving patient prognosis.

Methods

Cell Culture

The human breast cancer line MDA-MB-231 (MDA231) was authenticated by the Genomics Scientific Platform at i3S using the PowerPlex®16 HS System (Promega Corporation). Detection of the amplified fragments was made with automated capillary electrophoresis using the 3130 Genetic Analyzer (Applied Biosystems) and the assignment of genotypes was performed in GeneMapper software v5.0 (Applied Biosystems). The cells were cultured in Dulbecco's modified Eagle's medium, DMEM 1X (GIBCO, Paisley, UK) supplemented with 10% (V/V) heat-inactivated fetal bovine serum (FBS, Biowest, South American Origin) and 1X antibiotic solution penicillin-streptomycin, pen-strep (Gibco, Grand Island, USA), and maintained at 37 °C in a 5% CO_2 humidified atmosphere. Cells were used in experiments upon reaching 70–80% of confluence. The cells generated after the transfection assays were cultured in the same medium as MDA231 cells adding 700 µg/mL geneticin (Gibco, Thailand) for the maintenance of cell selection pressure. Note that, for the assays described bellow, the transfected cells were kept in complete medium without geneticin.

Stable Transfection Assay

To generate stable *HOXB7*-overexpressing and control cells, MDA231 were transfected with the pCMV6-AC-GFP-*HOXB7* (Origene, RG204495) or pCMV6-AC-GFP (Origene, PS100010) constructs. Transfections were performed using TurboFectin 8.0 (Origene) reagent according to manufacturer's instructions. Briefly, MDA231 cells were seeded in a 6-well plate on the previous day in order to get 50–70% confluence on the following day. The complexes formation were made in two different ratios, 1 µg DNA: 3 µl TurboFectin 8.0 and 1.5 µg DNA: 6 µl TurboFectin 8.0, and the transfected cells were incubated at 37 °C in a 5% CO_2

humidified atmosphere for 24 hours post-plating (h). After incubation, the cells medium was changed and geneticin (1.2 mg/mL) was added for the selection of the stably transfected cells. The GFP-positive/geneticin-resistant cells were then sorted in the FACSAria™ II cell sorter (BD Biosciences). Cells transfected with pCMV6-AC-GFP-HOXB7 plasmid vector were seeded in 96-well plate (1 cell/well) containing 20% FBS in order to achieve the clonal expansion of one cell and the remaining cells were collected in a T25 flask. The cells transfected with the empty vector (pCMV6-AC-GFP) were collected in a T25 flask with the conventional complete medium. Once cells restarted proliferation both in the T25 flask and in the 96-well plate they were kept in the conventional medium containing 700 µg/mL geneticin. Three different cell transfectants were obtained and named as Empty Vector (EV), for the cells transfected with the control empty vector (pCMV6-AC-GFP); B7, for the pool of cells transfected with pCMV6-AC-GFP-*HOXB7* vector and overexpressing variable levels of *HOXB7*; D3, for the clone obtained from the 96-well plate sorted cells transfected with pCMV6-AC-GFP-*HOXB7* vector.

RNA expression analyses

The total RNA extraction was performed using TRIzol™ reagent (Ambion, Carlsbad, USA) according to the manufacturer's instructions and adding one more wash with ethanol 75%. After assessment of RNA 260/280 nm ratio and concentration using NanoDrop 1000 (Thermo Scientific), 800 ng of RNA was subjected to reverse transcription, using the High-Capacity cDNA Reverse Transcription Kit (Applied Biosystems, Vilnius, Lithuania), following the manufacturer's instructions. The qPCRs reactions were performed in duplicates and carried out in the CFX96™ Real-Time PCR Detection System (Bio-Rad). Each 10µL amplification reaction contained 2µL of the respective cDNA diluted 1:4; the indicated quantity of forward and reverse 10 µM primers; 5µL of 2X iTaq™ Universal SYBR Green Supermix (Bio-Rad, USA) and 2µL of DNase/RNase free H_2O. The run conditions were: 95˚C for 3 minutes (min.), 40 cycles of 95˚C for 10 seconds (sec.) and 60˚C for 30sec. followed by the default dissociation curve capture. The qPCR result analyses were performed using the method described by Schmittgen and Livak [58] using the formula: RATIO = E target – (CT sample target gene) /E *GAPDH* – (CT sample GAPDH), in which "E" is the primer pair efficiency previously calculated and *GAPDH* (glyceraldehyde-3-phosphate dehydrogenate) is the reference gene. The primer sequences used for qPCR were synthetized by Sigma Aldrich (Darmstadt, Germany) and are described in Supplementary Table 1.

ChIP-qPCR assay

The cells were seeded in cell culture dishes with 15 cm in diameter in conventional medium and grown until reaching 80–90% confluence. Then, the DNA / proteins crosslink was performed using 1% formaldehyde solution incubation under agitation during 10 min. at room temperature. Next, to stop crosslink, 0.15M glycine was added directly onto the shaking plates and incubated for 5 min. at room temperature followed by two washes with cold 1X PBS (Gibco, Paisley, UK) and the cells were collected in 1.5 mL tubes after cell scrape. The obtained pellets, after 5 min. centrifugation at 1000 *g* at 4 °C, were suspended in Cell lysis buffer (5 mM Pipes, 85 mM KCl, 0.5% Igepal, 1X Roche cOmplete™ Protease Inhibitor Cocktail, 1 µL/mL Trypsin, 10 µL/mL PMSF 200 mM, 1 µL/mL DTT 50 mM in MilliQ H_2O) and incubated on ice for 10 min. followed by a centrifugation of 1000 *g* for 5 min. at 4 °C. The cell pellet was

suspended in Nuclear lysis buffer (50 mM Tris, 10 mM EDTA, 1% SDS 1X Roche cOmplete™ Protease Inhibitor Cocktail, 1 µL/mL Trypsin, 10 µL/mL PMSF 200 mM, 1 µL/mL DTT 50 mM in MilliQ H_2O), incubated for 10 min. on ice and immediately sonicated (30 cycles, 30 sec. ON/30 sec. OFF, high mode) in the Bioruptor Plus (Diagenode). The sonicated DNA (1 µg) fragment sizes were analysed in a 1% agarose gel with an expected smear under 1000 bp with a strong band at 500 bp. The DNA quantification was made in Nanodrop 1000 (Thermo Scientific) after the following preparation: 20 µl of sonicated samples was mixture in 20 µl of 10% Chelex® 100 resin (Bio-Rad, USA), incubated for 5 min. at 90 °C and centrifuged 15000 *g* for 1 min. The blank sample was prepared adding 20 µl of nuclear lysis buffer to 20 µl of 10% Chelex® 100 resin and following the same steps mentioned for the sample preparation. After DNA quantification and gel analyses, the sonicated DNA samples were heated for 5 min. at 65 °C and centrifuged 15000 *g* for 30 sec. Forty micrograms of DNA *per* Immunoprecipitation (IP) was diluted 1:20 in Dilution buffer (0.01% SDS, 1,1% Triton X-100, 1.2 mM EDTA pH 8.0, 16.7 mM Tris pH 8.1, 167 mM NaCl in MilliQ H_2O) and 4 µg of the desired antibody was added. The IPs were incubated overnight at 4 °C under rotation. An input control was prepared for each sample that was used diluting, also in a 1:20 ratio, 4 µg of each sample (10% of the IP) in Dilution buffer followed by the addition of 3 parts absolute ethanol and an overnight precipitation at -80 °C. On the day after, considering that 40 µl of Dynabeads A/G were used per IP, a mixture was prepared of 1 volume Dynabeads A and 1 volume Dynabeads G, followed by the beads separation with a magnetic stand, aspiration of the buffer and the addition of the same initial volume of IP buffer (10% Nuclear lysis buffer, 90% Dilution buffer). Next, the samples with antibodies were centrifuged for 10 min. at 12000 *g*, the supernatants were transferred to a new tube and 40 µl of Dynabeads preparation were added followed by an incubation for 2 h at 4 °C with rotation. The beads were, then, separated with a magnetic stand and washed (15 min. rotation at room temperature followed by beads separation) twice with 1 mL Dialysis buffer (2 mM EDTA pH 8.0, 50 mM Tris pH 8.1, 0.2% Sarkosyl in MilliQ H_2O) and four times with 1 mL Wash buffer (0.5 M LiCl, 1% Igepal, 1% Na-deoxycholate, 33.2 mM Tris pH 8.1 in MilliQ H_2O). After the last wash, beads were eluted in 150 µl Elution buffer (50 mM NaHCo3, 1% SDS), heated 15 min. at 65 °C with vortex each 5 min. and the supernatant transferred to a new tube. This step was repeated yielding 300 µl of supernatant per sample. The input controls were centrifuged 12000 *g* for 10 min. after the precipitation step and the pellets were washed twice with 70% ETOH (1 mL 70% ETOH and centrifugation), eluted with 300 µl Elution buffer and heated 15 min. at 65 °C with vortex every 5 min. To IPs and Input samples 2.4 µl Proteinase K (20 mg/mL) were added followed by 1 h incubation at 55 °C at 90 *g* and purification with QIAquick PCR purification kit (Qiagen, Hilden, Germany) according to manufacturer's instructions. Samples were suspended in DNase/RNase free H_2O and stored at -20 °C. The ChIP-qPCR reactions were performed using 2µL of the purified sample without dilution and the run conditions were: 95˚C for 3 min., 40 cycles of 95˚C for 15 sec., 55˚C for 30 sec. and 72˚C for 30 sec. followed by the default dissociation curve capture. The assays analyses were made using the "percent input" method according to Lacazette [42]. The primers sequences used for ChIP-qPCR were synthetized by Sigma Aldrich (Darmstadt, Germany) and are described in Supplementary Table 2.

Protein expression assays

Total protein extraction was obtained collecting the cells pellets after dissociation, suspending them in the lysis solution (0.1% Triton X-100, 0.1% Igepal, 1X cOmplete™ Protease Inhibitor Cocktail [Roche, Germany], PBS 1X [Gibco, Paisley, UK]) and incubating on ice for 20 min. with vortex every 5 min. After incubation, the tubes were centrifuged 9000 *g* for 10 min. at 4 °C and the supernatant transferred to a new tube. An aliquot of the protein extracts was separated for posterior quantification. Samples were stored at -80 °C.

Cytoplasmic and nuclear proteins fractions extractions were performed using the ab113474 Nuclear Extraction Kit (Abcam) according to the manufacturer's recommendations. The nuclear proteins fractions were sonicated in Bioruptor Plus (Diagenode) for 3 cycles, 10 seconds ON / 10 sec. OFF at high mode to increase extraction yield. Aliquots of both fractions were separated for posterior quantification. Samples were stored at -80 °C.

Protein concentrations were determined using the Pierce Detergent Compatible Bradford Assay Kit (Thermo Scientifc, Rockford, USA) following the product data sheet instructions. The albumin standards were prepared in a work range of 100–1500 µg/mL and the samples were quantified in a 1:10 dilution. Both, samples dilutions and albumin standards were prepared in RNase/DNase free H_2O. Twenty to thirty micrograms of protein lysates were separated on a 12% SDS-PAGE gel prepared with 40% Acrylamide – Bisacrylamide 29:1 (Invitrogen, Carlsbad, USA) and 4X separating buffer (Alfa Aesar, Ward Hill, USA) for the separating gel or 4X stacking buffer (Alfa Aesar, Karlsruhe, Germany) for the stacking gel. After run the proteins were blotted onto a nitrocellulose membrane of the iBlot® gel transfer stacks (Kiryat Shmona, Israel) using the iBlot™ dry transfer system (Life Technologies, Israel). Blots were blocked for 1 h at room temperature in 3% BSA/TBS-T (20 mM Tris, 137 mM NaCl, 0.1% Tween-20) solution or 5% skim milk/TBS-T solution and incubated overnight at 4 °C with the primary antibodies, diluted in the respective blocking solutions. Then, membranes were washed four times in TBS-T for 5 min., two times in TBS (20 mM Tris, 137 mM NaCl) for 5 min. and incubated with the appropriate horseradish peroxidase-conjugated secondary IgG antibody for 1.30 min. at room temperature. The bolts were washed again, as already described, followed by the detection of the immunoreactive proteins using the Clarity™ Western ECL Substrate (Bio-Rad, USA) in the ChemiDoc Gel Image System (Bio-Rad). The primary and secondary antibodies used in this work are listed on Supplementary Table 3. The assessment of the bands density was made in the ImageLab software (BioRad) using the measures of Tubulin (for total and cytoplasmic protein fractions) and HDAC1/Lamin B1 (for nuclear protein fraction) as loading controls.

MTT assay with docetaxel treatments

Cell viability was determined using MTT assay [3-(4,5-dimethylthiazol-2yl)-2,5-diphenyltetrazolium bromide] (EMD Millipore, China) following the manufacturer's instructions. Cells were seeded in 96-well plates (1×10^4 cells/well) and maintained at 37 °C in 5% CO2 humidified atmosphere in complete media supplemented with 5% FBS for 24 h. In this time point (24 h), the Docetaxel (Sigma-Aldrich, China) treatments with 5 nM and 50 nM started. The cells viability measures were made by absorbance read at 570 nm using the Synergy™ 2 Plate reader (BioTek) at 24 h, 48 h, 72 h and 96 h post-seed. The medium

containing Docetaxel or vehicle (ETOH) was changed every 24 h to ensure that cells were exposed to the same drug concentration along of time points analysed. The control cells were treated with the drug vehicle (ETOH) in the volume corresponding to the biggest drug concentration used. An additional assay was made for the measure of the cell viability in standard medium without ETOH.

On-top 3D cell culture

For the morphogenesis assay, MDA231 wild-type (WT), EV and D3 cells were dissociated to obtain a suspension containing single cells. The cells (2×10^3), suspended in 400 µL of completed media containing 3% of Matrigel® Matrix Basement Membrane growth factor reduced (Corning, Bedford, USA), were seeded in 8-well glass chamber slides containing a pre-prepared bed of 30 µl Matrigel® Matrix Basement Membrane growth factor reduced, as described by Debnath *et al.* [24] and incubated at 37 °C in 5% CO2 humidified atmosphere for 8 days. The cells spheroids morphologies were analysed and registered every two-days in Axiovert 200M inverted fluorescent microscope (Carl Zeiss). On day-4, 100 µl of media containing 3% Matrigel® Matrix Basement Membrane growth factor reduced were added to the wells to prevent the effects of medium evaporation and nutrient scarcity.

Wound Healing assay

Cells were seeded in 24-well plates at a density of 2×10^5 cells/well in 500 µl of Dulbecco's modified Eagle's medium, DMEM 1X (GIBCO, Paisley, UK) supplemented with 5% (V/V) Charcoal Stripped Fetal Bovine Serum Qualified One Shot™ (Gibco, Mexico), for cells mitosis synchronization, and 1X antibiotic solution penicillin-streptomycin (pen-strep, Gibco™). At least 48 h post-seed, to ensure cell synchronization and growth to 90%-100% confluence, a single scratch wound was made in each well using a 200 µl disposable pipette tip. The cells were then incubated for 15 h in the InCell Analyser 2000 Automated fluorescence widefield HCS microscope for the capture of wound images every 3 h. The extent of wound closure was measured using the MRI wound healing tool from ImageJ software [59].

Invasion assay

The invasion assay was made using the 24-well plate growth factor reduced Corning® Matrigel® Invasion chambers 8 µm pore size (Corning, Bedford, USA) and 24-well Control Inserts 8 µm pore size (Corning, Bedford, USA) according to manufacturer's instructions. Briefly, cells (1×10^5) in 500 µl serum-free medium were plated into the upper chamber and the bottom wells were filled with 750 µl complete medium. The cells were incubated at 37 °C in 5% CO2 humidified atmosphere for 16 h. Then, cells in the upper chamber were removed using cotton swabs and the cells invading the bottom of the membrane were fixed with 4% paraformaldehyde for 20 min. The nuclei were stained with DAPI (Sigma-Aldrich, Darmstadt, Germany) 1 µg/mL plus 1% Triton X-100 in 1X PBS (Gibco, Paisley, UK) for 15 min. followed by two washes in Milli-Q H_2O. Ten random fields from each membrane were photographed using the Zoe fluorescent cell imager (Bio-Rad) and the cells nuclei were counted using the Analyze Particles tool from ImageJ software [59].

Clonogenic assay

Clonogenic assay is a versatile tool for *in vitro* screening of the capacity of a single-cell suspension to form a colony of 50 or more cells under different circumstances. The assay was made according to Franken *et al*. [26]. A total of 100 cells were seeded into 6-well plates containing standard culture media. After 10 days, colonies were stained and the well images captured in the InCell Analyser 2000 Automated fluorescence widefield HCS microscope. Colony number and respective areas were measured using the colony count plugin from ImageJ software [59].

Soft agar colony formation assay

This assay was made as described by Borowicz and colleagues [7]. The cells (1.5×10^4/well) were seeded in 6-well plates and incubated for four weeks at 37 °C in a 5% CO2 humidified atmosphere. The colonies, without staining, of nine random fields were counted using the Zoe fluorescent cell imager (Bio-Rad). MCF7 cells cultured in the same medium as MDA231 cell linewere used as a parameter for Luminal behavior analyses.

Slow Aggregation Assay

This assay was performed according to the protocol described by Boterberg *et al* [8]. Briefly, 2×10^4 cells per well were seeded over an agar layer in a 96-well plate with and without the addition of MB2, an anti-CDH1 antibody, as a way to show if the formed aggregates are dependent on the CDH1/CTNNB1 complex functionality. The cells were photographed after 24 h, 48 h, 72 h and 96 h in an Axiovert 200M inverted fluorescent microscope (Carl Zeiss). The MDA231-WT and MCF7 cells were used, respectively, as negative and positive controls of the aggregation capacity. MDA231-WT cells do not express CDH1 and, therefore, they do not aggregate while MCF7 cells, which express high levels of CDH1, form well-defined aggregates when CDH1/CTNNB1 complex is active.

Statistical analyses

The statistical differences were determined by unpaired T test with Welch's correction or by Brown-Forsythe and Welch ANOVA tests using the Prism8 software (GraphPad Software, La Jolla, USA). *P*-values were considered statistically significant when $P \leq 0.05$. Data were reported as the mean ± SD of at least three independent experiments.

Results

1. HOXB7 overexpression induced in MDA231 cells

HOXB7 is typically overexpressed in breast cancer cell lines in comparison with normal cells [15]. However, the level of *HOXB7* overexpression is lower in MDA231 cells (triple-negative, claudin-low) in comparison to MCF7 (Luminal A), BT474 (Luminal B), SKBR3 (HER2+) and MDA468 (Triple-negative, basal-like). Thus, we selected the MDA231 cell line to conduct functional assays aiming to further explore the mechanistic effect of *HOXB7* up-regulation. To this end, we transfected these cells with pCMV6-AC-GFP plasmid vector as control generating the EV (Empty Vector) cells and with pCMV6-AC-GFP-HOXB7 plasmid vector generating the B7 and D3 cells.

Subsequent mRNA expression analysis revealed that the levels of *HOXB7* were identical in EV and WT cells, suggesting that the transfection procedure does not affect *HOXB7* expression (Fig. 1A). In contrast, the B7 and D3 cells presented a significantly higher *HOXB7* mRNA expression levels (P = 0.02 and P = 0.013, respectively) when compared to EV cells. In addition, the *HOXB7* expression was significantly higher in the D3 than in the B7 cells (P = 0.015). Noteworthy, in terms of protein expression, we observed that HOXB7 levels did not change among WT, EV, B7 and D3 cells in the cytoplasmic fraction (Fig. 1B). However, in the nuclear fraction (Fig. 1C), HOXB7 expression was significantly higher only in D3 cells, in comparison with EV (P = 0.026), with a borderline significance in B7 (P = 0.049) cells. Thus, in summary, we confirmed that pCMV6-AC-GFP-HOXB7 transfection led to mRNA *HOXB7* overexpression in B7 and D3 cells, and we further detected that only D3 cells present significant HOXB7 overexpression at nuclear protein level.

2. Phenotypic characterization of the HOXB7**-overexpressing cells**

2.1 More compact spheroid organizations in 3D culture

The three-dimensional (3D) culture on a reconstituted basement membrane results in formation of spheroids that recapitulate several aspects of glandular architecture *in vivo* [24]. The morphology of B7 and D3 cell growth in the conventional 2D culture did not show impacting differences in comparison to the morphology observed in WT and EV cells (Supplementary Fig. 1). However, we hypothesized that 3D cellular organization could be different in the *HOXB7* overexpressing cells. To address this question, the cells were grown on-top in Matrigel® for 8 days (Fig. 2), which allowed us to see that D3 cells form spheroids with a more compact growth without the formation of protrusions. In contrast, WT, EV and B7 cells showed a more spread growth with numerous protrusion formations. Interestingly, the spheroids growth pattern of D3 cells resembles that observed for MCF7 cells (Luminal A) as shown by Tasdemir *et al.* [64] and Kai *et al*. [34].

2.2 Lower cell viability and no effect on sensitivity to Docetaxel treatments

The effect of *HOXB7* overexpression on cell viability and Docetaxel sensitivity was analysed in WT, EV, B7 and D3 cells by MTT assay at different time points (Fig. 3). At 48 h post-plating, the D3 cells exhibited lower viability in comparison to EV (P = 0.002) and B7 (P = 0.015) cells (Fig. 3A). The B7 (P = 0.001) and D3 (P = 0.0001) cells showed a lower viability in comparison to EV cells at 96hpost-plating. However, these differences in 96 h could lead to misinterpretations because at this time-point the cells were in a confluence near 100%. We then evaluated the sensitivity to Docetaxel, a chemotherapeutic drug that induces different types of cell death depending on the administrated concentration [30]. We observed that, in the presence of Docetaxel (5 nM and 50 nM), the cells do not reach the exponential growth as observed in absence of the drug (Fig. 3B). The viability differences observed at 24 h post-plating (time 0 h for drug treatments) among the cells before and after Docetaxel treatment are probably related to cell loading and/or cell attachment issues. Despite the differences in 24 h, it is possible to observe the lower viability

of the D3 cells kept with ETOH in 96 h compared to EV (P = 0.005) and B7 (P = 0.003) cells corroborating the findings of the curve in Fig. 3A. In the ETOH assay the cells were sub confluent at 96 h, possibly due to the differences observed at 24 h. Thus, no differences in response to Docetaxel treatments were observed over time.

2.3 Lower migration and invasion capacities

The cell migration capacity is essential for disease progression and is considered the first step for lymphovascular invasion and tumour metastasis [37]. The data obtained by wound-healing assay showed that D3 cells had a significant delay in wound closure capacity in all analysed time points when compared to EV and B7 cells (Fig. 4). It is interesting to note that at time 0 h there are significant differences between EVxB7 (P < 0.0001) and B7xD3 (P = 0.0001) cells. This could be due to differences in the areas of the opened wounds. The EVxB7 differences decrease along the time (P = 0.0004 at 3 h) and disappear after 6 h, while the B7xD3 (P < 0.0001) as well as the EVxD3 differences were kept throughout the assay (P = 0.027 at 3 h and P < 0.0001 at 6 h, 9 h, 12 h and 15 h). The invasion capacity, which is another important skill developed by cancer cells to successfully spread locally and for distant sites, was analysed by Matrigel® invasion chamber assay. It was observed that D3 cells present lower capacity (P = 0.004) to invade the Matrigel® layer in comparison to EV cells with an invasion index of 0.4 (Fig. 5), which means that D3 cells invasion capacity is approximately 60% less than in EV cells.

2.4 Lower soft agar colony formation efficiency with no changes on clonogenic growth

The ability of the transformed cells to grow and form colonies independently of a solid surface is a hallmark of carcinogenesis [7]. This capacity was evaluated in the soft agar colony formation assay and it was observed that D3 cells formed significantly less colonies than WT (P = 0.041) and EV (P = 0.007) cells (Fig. 6). Moreover, when compared to a Luminal A cell line (MCF7), MDA231 WT and EV cells showed a higher number of colonies (P = 0.009 and P = 0.007, respectively), while D3 cells showed a colony number similar to MCF7 cells. In summary, D3 cells presented a colony formation efficiency that represents about 50% of the efficiencies observed in WT and EV cells, which is similar to what is observed in MCF7 cells. We also evaluated the capacity of a single cell to form progeny in an attachment-permissive environment by the clonogenic assay and it was observed that, in this condition, the clonogenic capacity of EV and D3 is similar both in the number and area of the colonies formed (Supplementary Fig. 2).

3. Potential downstream targets

3.1 Impact on CTNNB1 expression

The current knowledge on the direct and/or indirect targets of HOXB7 is scarce; therefore, the search for these molecules is crucial to better understand HOXB7 functions in different tumours. Given the results

obtained in 3D culture, showing a more compact and organised spheroid formation in D3 cells, we speculate that molecules involved in cell-cell adhesion and cytoskeletal organization (*i.e.* CDH1/CTNNB1 complex) could be influenced by *HOXB7* overexpression. In this line of thought, we performed a slow aggregation assay in order to verify if the phenotypes mentioned above could be related to changes in CDH1 functionality, given that MDA231 cells do not express CDH1 and consequently do not form aggregates in this assay. However, no alterations were observed in the D3 cell aggregation profiles, in the presence and absence of MB2 antibody, in comparison to WT and EV cells (Supplementary Fig. 3), and the phenotypes observed in 3D cell culture were not directly linked to variations in CDH1 activity.

Next, we analysed the expression of *CTNNB1*, a multi-functional molecule with key roles in normal and disease conditions [8]. Interestingly, we found a significant downregulation of *CTNNB1* mRNA (P = 0.021, Fig. 7A) and total protein (P = 0.007, Fig. 7B-C) in D3 cells.

3.2 HOXB7 interacts with CDH1, FGF2 and CTNNB1 promoter regions and, when overexpressed, EGFR, DNMT3B and COMMD7 genes become new targets

Based on previous studies, several putative targets of HOXB7 may explain its mechanistic role when overexpressed in breast cancer cells: *EGFR, FGF2, CTNNB1, CDH1, DNMT3B* and *COMMD7*. HOXB7 seems to establish direct interactions with EGFR in MCF7 [32] and BT474 cells [29] and with FGF2 in BT474 cells [29]. In addition, the knockdown of *CTNNB1* in TNBC cell lines (MDA231 and HCC38) significantly impairs their ability to migrate and form anchorage-independent colonies [68] besides showing a down-regulation in our *HOXB7*-overexpressing cells (Fig. 7). Moreover, reduced expression of CDH1 is linked to the invasion capacity of cancer cells [19]; however its interaction with HOXB7 has not been explored in breast cancer cells. Regarding *DNMT3B*, its function relates to *de novo* methylation, which has an important impact on epigenetic regulation of several genes [48] and TNBC prognosis [50]. It was also shown that HOXB7 binds directly to T*GFB2* promoter in MCF7 cells and upregulates this same molecule in MDA231 cells leading to increased cell migration and invasion [17]. Finally, the analysis of ChIP-Seq data provided by Heinonen *et al.* [29] suggests that *COMMD7* might be a direct target of HOXB7 in BT474 cells (Supplementary Fig. 4A), as its function is explored in the progression of hepatocellular [70] and pancreatic carcinomas[69]. Here we analysed *COMMD7* expression in a panel of breast cancer cells and found up-regulation in BT474 and MDA231 (Supplementary Fig. 4B). We then used ChIP-qPCR to explore the interaction of HOXB7 with all putative targets mentioned above. We detected three HOXB7 interaction patterns (Fig. 8): 1) interaction in EV and D3 cells with no increments in D3 cells for *CTNNB1* and *FGF2*; 2) interaction only in D3 cells for *EGFR*, *DNMT3B* and *COMMD7*; and 3) interaction in EV and D3 cells with an increment in D3 cells for *CDH1*. No interactions between HOXB7 and *TGFB2* were found in EV or D3 cells. The calculated P values are described in the legend of Fig. 8.

Discussion

Triple-negative breast cancers (TNBC) corresponds to up to 15% of the total breast cancer cases and have the worse prognosis among breast cancer subtypes due to the absence of target-directed therapies and the increased rate of distant metastasis [41, 45, 54]. As reviewed by de Bessa Garcia *et al*, *HOXB7* has been frequently considered as an oncogene in breast cancer [22]. However, our analyses of the *HOXB7* basal mRNA expression profile [27] showed that the lowest levels were observed in SKBR3 (HER2+) and MDA231 (TNBC, claudin-low) cells, which represent the molecular subtypes with worse prognosis, while the highest expression levels were observed in the luminal A and B cells (MCF7 and BT474, respectively), representing tumour molecular sub-types with better prognosis [52]. Surprisingly, the MDA231 cells overexpressing *HOXB7* mRNA and nuclear protein showed less aggressive phenotypes, represented by more compact spheroid formation in 3D culture and lower cell viability, migration, invasion and anchorage-independent colony formation. Moreover, the search for potential downstream targets showed that the *HOXB7*-overexpressing cells, along with a decreased *CTNNB1* expression, present enriched HOXB7 protein direct interaction with the promoter regions of *EGFR*, *DNMT3B*, *COMMD7* and *CDH1* genes.

The culture of breast cells on a reconstituted basement membrane results in a 3D-growth that recapitulates several aspects of glandular architecture *in vivo* that are lost in 2D culture, as demonstrated with MCF10A cells [21, 24]. Interestingly, MDA231 *HOXB7*-overexpressing cells (D3) formed compact spheroids compared to the spread and branched growth shown by MDA231 EV cells. When cultured in 2D conditions, the EV and D3 cells did not show impacting differences in their morphology. Moreover, the spheroids of MDA231 HOXB7-overexpressing cells resembled those generated by BT474 and MCF7 cells [34, 43], reinforcing the idea that *HOXB7* up-regulation should be related to a more luminal phenotype.

The plasma membrane protrusions are the result of the continuous synthesis and remodelling of the cytoskeleton actin filaments and are closely related to the promotion and driving of cell migration. The formation of protrusions occurs in both 2D and 3D cell migration. In 3D cell movement, these protrusions are collectively known as invadossomes that establish close contact with the ECM (Extracellular Matrix) and perform a proteolytic matrix degradation to invade the connective tissues [36]. Thus, the decreased protrusions formation observed in 3D culture could explain the impaired capacity of *HOXB7*-overexpressing cells to migrate in a 2D culture and to invade through the Matrigel® matrix as will be discussed in detail ahead.

The impact of *HOXB7* overexpression on breast cancer cell proliferation has been demonstrated in different cellular models. Caré *et al* [16] showed that *HOXB7* overexpression in SKBR3 cells (ER-/PR-/HER2+) leads to increased cell proliferation through the up-regulation of *FGF2*. Ma *et al* [49] corroborated these results in MCF7 cells (ER+/PR+/HER2-) in which *HOXB7* down-regulation decreased the proliferation ratios. However, an *in vivo* study conducted by Chen *et al* [18] showed that the *HOXB7* overexpression alone was insufficient to induce tumour formation and had a dual role when co-overexpressed with HER2. The Hoxb7/Her2 transgenic mice, compared to Her2 transgenic animals, showed a delayed tumour onset reflected in a decreased tumour multiplicity but, once the tumour was

established, Hoxb7 promoted tumour progression leading to the formation of larger masses and to a higher index of pulmonary micrometastasis. Additionally, *in silico* analyses of public microarray data showed that high level of *HOXB7* predict a poor outcome in HER2-positive, but not in HER2-negative breast cancers [18]. Therefore, this is a strong indication that the HOXB7 role in tumour progression is dependent on the cellular genetic background, especially concerning the HER2 profile and ECM interactions.

The cell/cell and cell/ECM interactions are important for cellular architectural maintenance and growth control among other processes [56]. To metastasize, breast cancer cells must detach from the tumour mass and resist to *anoikis*, a programmed cell death induced by lack of cell/ECM communication [5]. The MDA231 cell line was established from cells recovered from a patient's pleural effusion [14]. Therefore, these cells had already accomplished the entire metastization process and, additionally, maintained its metastatic capability in *in vivo* mouse models. Here, we showed that *HOXB7* overexpression leads to a decreased capacity of colony formation in an anchorage-independent environment. Moreover, *HOXB7* overexpressing cells showed a capacity similar to that observed in MCF-7 cells, which is also a cell line established from a pleural effusion but non-metastatic *in vivo*. Akekawatchai *et al* [1], through proteomic analyses, identified 54 proteins that were expressed only in suspended and adherent MDA231 but not in MCF-7 cells in the same conditions. Could MDA231 *HOXB7*-overexpression have change the expression profiles of some proteins in order to have a genetic background more similar to the MCF7 cells? Could these proteins be related to the other phenotypic changes observed? These questions deserve attention. Controversially, the *HOXB7*-overexpression in SKBR3 cells (HER2+) increased their ability to form colonies in semisolid medium [16]. Once again, the contradictory findings could be related to the different genetic profile of the cells and consequently to the pathways modulated in each particular condition. Thus, characterization of the HOXB7 targets is an urgent issue for better understanding of the HOXB7 functions in different cellular contexts. In this study, we investigate the physical interaction between HOXB7 protein and the promoter regions of the genes *EGFR, DNMT3B, CDH1, CTNNB1, FGF2, TGFB2* and *COMMD7*.

The EGFR (Epidermal Growth Factor Receptor) overexpression is recognized as a driver mechanism in the initiation, progression and therapy resistance of several carcinomas such as lung, breast and pancreatic cancers [3], being the interaction between HOXB7 and the *EGFR* promoter region already demonstrated [29]. EGFR is also an important target in multiple chemotherapeutic regimens [13]. It is a member of ERBB family, which is composed of ERBB-1 (HER1/EGFR), ERBB-2 (HER2), ERBB-3 (HER3) and ERBB-4 (HER4) receptors, and are activated when in dimers after ligand-binding [55]. Jin *et al* [32] showed that tamoxifen resistance in MCF7 cells is related to a progressive increasing in *HOXB7* expression levels, along with the up-regulation of EGFR and its ligands. Making a parallel between the genetic backgrounds of MDA231 and MCF7 cells concerning HOXB7, EGFR and ER expression [20, 27, 61], we can infer that MDA231 is HOXB7-low, EGFR-high and ER-negative, while MCF7 is HOXB7-high, EGFR-low, and ER-positive. Therefore, in both cells, we observed an inverse correlation among the three molecules. Additionally, BT474 cells are HOXB7-high, EGFR-intermediary, ER-positive, but resistant to hormone therapy. Noteworthy, BT474 cells also express intermediary levels of HER2 for which EGFR is the preferred dimer-

partner. Added to our finding that HOXB7/EGFR interaction occurred only in *HOXB7*-overexpressing MDA231 cells (HOXB7-high, EGFR-high, ER-negative) this is are supplementary evidence that HOXB7 action is dependent, not only on its own expression, but also on the molecules that are active in the cell, named ER, EGFR and HER2. Thus, different genetic profile combinations could lead to different responses for the same stimulus in the same tissue.

The interaction between HOXB7/DNMT3B was only observed in *HOXB7*-overexpressing cells as the case of *EGFR*. No studies exist correlating HOXB7 and DNMT3B molecules. However, it is widely known that the levels of DNMTs, especially of DNMT3B, DNMT3A, and DNMT3L, are often increased in various cancer tissues and cell lines, and may account for the hypermethylation of tumour suppressor genes in a variety of malignancies [62]. As the HOXB7 methylation, which have already been described in several cancers and shown to be related to patients' prognosis [53], the search for genes that are hypermethylated in response to *HOXB7*-binding to DNMT3B is also an important and interesting approach to pursue.

CDH1 was another gene shown to interact with HOXB7 in MDA231 cells with an interaction increment in those overexpressing *HOXB7*. It was already demonstrated that *HOXB7*-overexpression in MCF10A cells, causes a reduction on CDH1 protein expression [67]. In breast cancer, deregulation of the CDH1 function plays crucial roles in metastases and is related to worse prognosis and shorter overall survival of patients [19]. Despite the higher HOXB7/CDH1 interaction found in MDA231 HOXB7-overexpressing cells, the CDH1 functionality did not change between EV and D3 cells, as accessed by the aggregation assay. However, CDH1 interacts with the actin cytoskeleton [19] and therefore the increment of the HOXB7/CDH1 interaction in MDA231 *HOXB7*-overexpressing cells could be related with the absence of protrusion formations in these cells. Additionally, CDH1 works in complex with CTNNB1 to ensure cell–cell adhesion between epithelial cells [8]. The balance between CDH1 and CTNNB1 expression is responsible for the cell adherens-junction maintenance or for the CTNNB1 release from the complex followed by its degradation or nuclear translocation, where it forms complexes with members of the TCF/LEF family to activate the transcription of target genes involved in self-renewal, EMT (Epithelial to Mesenchymal Transition) and cell proliferation [51, 65]. Moreover, in breast cancer patients, nuclear and cytosolic accumulation of CTNNB1, but not the membrane-associated form, is associated with reduced overall survival [38].

To our surprise, the *CTNNB1* promoter region showed to be a HOXB7 target in MDA231 EV and D3 cells, adding the fact that the CTNNB1 mRNA and protein levels were decreased in *HOXB7*-overexpressing cells. Xu *et al* [68] demonstrated that CTNNB1-knockdown impaired the ability of the MDA231 and HCC38 cells to migrate. Moreover, the HCC38 cells showed a decreased capacity to form anchorage-independent colonies in soft agar, a lower stemness potential and a reduced tumorigenic potential *in vivo* and an increased sensitivity to chemotherapeutic agents (cisplatin and doxorubicin). Another study by Lin and colleagues [46] showed that the CTNNB1 downregulation, promoted by luteolin treatment, effectively reverses EMT in the MDA231 and BT549 TNBC cells and suppresses the metastatic potential of MDA231 cells *in vivo*. These findings could be related to the phenotypes of migration and invasion observed in D3 cells. Concerning the stemness, we analysed the mRNA expression of the c-*Myc*, *NANOG*, *OCT4*, and

SOX2 transcription factors, known as master regulators of pluripotency and stemness [63], and did not observe any differences between EV and D3 cells (Supplementary Fig. 5). This could be due to the fact that the signals released by CTNNB1 knockdown to promote changes in stemness are not the same as those provided by the *HOXB7* overexpression effects on *CTNNB1* expression. The same explanations could be applied to the absence of sensitivity changes to docetaxel treatments. The chemotherapeutic drugs have different action modes and different mechanisms of resistance. Cisplatin and doxorubicin are DNA-interfering drugs, while docetaxel acts on tubulin impairing the microtubules dynamics and consequently, inhibiting cell cycle progression [39, 60].

Another gene that showed a direct interaction with HOXB7 in both EV and D3 cells was *FGF2*. The HOXB7/FGF2 interaction has already been described in melanoma cell lines [15] and in BT474 breast cancer cell line [29]. Moreover, when the coordinated expression of HOXB7 and FGF2 was demonstrated in melanomas, glioblastomas and leukemias, it was also shown that SKBR3 (HER2+) cells are negative for HOXB7 and FGF2 expression [16]. We found that *FGF2* is expressed only in MCF10A (normal breast) and MDA468 (TNBC, basal) cells (Supplementary Fig. 6). Even in MCF7, BT474 and D3 cells, which show high levels of *HOXB7*, the *FGF2* expression was undetectable (Supplementary Fig. 6). Despite the existence of HOXB7/FGF2 interaction in different cell models and the described relationship between the increased expression of *FGF2* in breast cancer [6], further studies are needed to establish in which context HOXB7 may be involved in *FGF2* expression regulation.

Although the HOXB7 direct binding to the activation of *TGFB2* promoter has already been described in MCF7 cells [47], this interaction was not observed in MDA231 EV and D3 cells. Liu and colleagues [47] showed that the knockdown of *TGFB2* leads to a decrease in the migration and invasion capacities of MDA231 cells overexpressing *HOXB7*, along with a dramatic inhibition of lung metastasis formation in an *in vivo* model. The *TGFB2* mRNA levels were also analysed in EV and D3 cells but no differences were detected (Supplementary Fig. 7). The role of TGFB2 in breast cancer progression is ambiguous, since it was shown to display tumour-suppressing and -enhancing effects. [2, 11, 72]. Thus, a number of questions still need to be addressed in order to completely understand the regulation of TGFB2 and its interaction with pathways activated in the course of tumour progression.

Finally, *COMMD7*, a gene that we found to be overexpressed in BT474 and MDA231 breast cancer cell lines (Supplementary Fig. 4) and that potentially presents enriched interactions with HOXB7 in BT474 [29], was found to bind to a target of HOXB7 in D3 cells. The COMMD family is a group of proteins that act as scaffold proteins to facilitate the assembling of crucial molecules involved in the control of several biological processes such as the NF-κB signalling [25]. No information exists on the specific role of COMMD7 in breast cancer but data exists revealing that *COMMD7* expression levels are up-regulated in hepatocellular carcinoma tissues [71] and in pancreatic ductal adenocarcinoma (PDAC) tissues and cell lines [43]. Interestingly, *HOXB7* expression is also high in liver and pancreatic tissues, as reviewed by de Bessa Garcia and colleagues [22]. Therefore, it is possible to infer that HOXB7 and COMMD7 could have

correlated and interaction-dependent functions not only in breast cancer, but also in other cancers. A summary of the main findings of this work is represented in the scheme shown in Fig. 9.

Conclusion

Triple Negative breast cancer cells expressing high levels of *HOXB7* mRNA and nuclear protein show a less aggressive phenotype represented by lower viability and decreased migration, invasion and anchorage-independent colony formation capacities along with a more compact spheroid formation in 3D culture. In MDA231 cells overexpressing *HOXB7*, the HOXB7 protein interacts with *CTNNB1*, *FGF2*, *CDH1*, *EGFR*, *DNMT3B* and *COMMD7* promoter regions. Moreover, these cells present *CTNNB1* down-regulation, which relates with the phenotypes observed. Thus, the present study raises important questions concerning, not only the downstream targets of HOXB7, but also the molecules that could be involved in *HOXB7* regulation and nuclear translocation as well as the genes that are differentially methylated in response to HOXB7/DNMT3B interaction. In addition, our results suggest that the HOXB7 role in breast cancer is strictly dependent on the cellular genetic background, especially concerning ER, EGFR and HER2 expression, and modulated by the transcriptional levels of this transcription factor.

Abbreviations

2D- Two-dimensional

3D- Three-dimensional

ECM- Extracellular Matrix

ER- Estrogen receptor

ETOH - Ethanol

EV- Empty Vector

FBS- Fetal Bovine Serum

g- gravitational force equivalent

h- hours

IP- Immunoprecipitation

min.- minutes

PR- Progesterone receptor

sec.- seconds

TNBC- Triple Negative Breast Cancer

V/V- volume/volume

WT- Wild-Type

Declarations

Ethical approval and consent to participate

No applicable

Consent for publication

No applicable

Availability of data and material

The datasets used and/or analyzed during the current study are available from the corresponding author on reasonable request.

Competing interests

The authors declare no competing interests

Funding

FEDER - Fundo Europeu de Desenvolvimento Regional funds through the COMPETE 2020 - Operacional Programme for Competitiveness and Internationalisation (POCI), Portugal 2020, and Portuguese funds through FCT - Fundação para a Ciência e a Tecnologia/Ministério da Ciência, Tecnologia e Ensino Superior in the framework of the project POCI-01-0145-FEDER-030562 (PTDC/BTM-TEC/30562/2017).

Authors' contributions

SABG and RF designed the study, SABG executed the assays, performed data interpretation and wrote the manuscript, MA performed the COMMD7 qPCR and *in silico* analyses, TP performed the expression analyses of stemness markers, *CTNNB1*, *FGF2* and *TGFB2*. RF provided financial support, discussed results, participated in the writing of the manuscript and supervised the work.

Acknowledgments

We acknowledge Barbara Sousa for the assistance in the aggregation assay protocol, Joana Paredes for kindly provide the MDA-MB-231 cells and the MB2 antibody, Carmen Jerónimo for kindly provide the additional breast cancer cell lines. We are grateful to Ana Paço for participating in the preliminary data collection and Raul Guizzo for editing assistance and proofreading. We also acknowledge the i3S

scientific platforms (https://www.i3s.up.pt/scientific-platforms) for technical support and equipment provided: 1) Biochemical and Biophysical Technologies (b2Tech), NanoDrop 1000 (Thermo Scientific) and Bioruptor Plus (Diagenode); 2) Bioimaging (member of the national infrastructure PPBI - Portuguese Platform of Bioimaging, PPBI-POCI-01-0145-FEDER-022122), Axiovert 200M inverted fluorescent microscope (Carl Zeiss); 3) BioSciences Screening (member of the national infrastructure PPBI - Portuguese Platform of Bioimaging, PPBI-POCI-01-0145-FEDER-022122), Synergy™ 2 Plate reader (BioTek) and InCell Analyser 2000 Automated fluorescence widefield HCS microscope; **4) Cell Culture and Genotyping (CCGen), cell culture room,** CFX96™ Real-Time PCR Detection System (Bio-Rad), ChemiDoc Gel Image System (Bio-Rad) and Zoe fluorescent cell imager (Bio-Rad)**;** 5) Translational Cytometry Unit, TraCy (project MICROXXI - NORTE-07-0162-FEDER-000033 funded by ON2), FACSAria™ II cell sorter (BD Biosciences).

References

1 Akekawatchai C, Roytrakul S, Kittisenachai S, Isarankura-Na-Ayudhya P, Jitrapakdee S (2016). Protein Profiles Associated with Anoikis Resistance of Metastatic MDA-MB-231 Breast Cancer Cells. *Asian Pacific journal of cancer prevention : APJCP***17:** 581-590.

2 Beisner J, Buck MB, Fritz P, Dippon J, Schwab M, Brauch H *et al* (2006). A novel functional polymorphism in the transforming growth factor-beta2 gene promoter and tumor progression in breast cancer. *Cancer research***66:** 7554-7561.

3 Bhatia P, Sharma V, Alam O, Manaithiya A, Alam P, Kahksha *et al* (2020). Novel quinazoline-based EGFR kinase inhibitors: A review focussing on SAR and molecular docking studies (2015-2019). *European journal of medicinal chemistry***204:** 112640.

4 Bhatlekar S, Fields JZ, Boman BM (2014). HOX genes and their role in the development of human cancers. *J Mol Med (Berl)***92:** 811-823.

5 Bizjak M, Malavašič P, Dolinar K, Pohar J, Pirkmajer S, Pavlin M (2017). Combined treatment with Metformin and 2-deoxy glucose induces detachment of viable MDA-MB-231 breast cancer cells in vitro. *Scientific reports***7:** 1761.

6 Blanckaert VD, Hebbar M, Louchez MM, Vilain MO, Schelling ME, Peyrat JP (1998). Basic fibroblast growth factor receptors and their prognostic value in human breast cancer. *Clinical cancer research : an official journal of the American Association for Cancer Research***4:** 2939-2947.

7 Borowicz S, Van Scoyk M, Avasarala S, Karuppusamy Rathinam MK, Tauler J, Bikkavilli RK *et al* (2014). The soft agar colony formation assay. *J Vis Exp***:** e51998-e51998.

8 Boterberg T, Bracke ME, Bruyneel EA, Mareel MM (2001). Cell aggregation assays. *Methods in molecular medicine***58:** 33-45.

9 Bray F, Ferlay J, Soerjomataram I, Siegel RL, Torre LA, Jemal A (2018). Global cancer statistics 2018: GLOBOCAN estimates of incidence and mortality worldwide for 36 cancers in 185 countries. *CA: a cancer journal for clinicians***68:** 394-424.

10 Brotto DB, Siena Á DD, de B, II, Carvalho S, Muys BR, Goedert L *et al* (2020). Contributions of HOX genes to cancer hallmarks: Enrichment pathway analysis and review. *Tumour biology : the journal of the International Society for Oncodevelopmental Biology and Medicine***42:** 1010428320918050.

11 Buck MB, Knabbe C (2006). TGF-beta signaling in breast cancer. *Annals of the New York Academy of Sciences***1089:** 119-126.

12 Burglin TR, Affolter M (2016). Homeodomain proteins: an update. *Chromosoma***125:** 497-521.

13 Cai WQ, Zeng LS, Wang LF, Wang YY, Cheng JT, Zhang Y *et al* (2020). The Latest Battles Between EGFR Monoclonal Antibodies and Resistant Tumor Cells. *Frontiers in oncology***10:** 1249.

14 Cailleau R, Young R, Olivé M, Reeves WJ, Jr. (1974). Breast tumor cell lines from pleural effusions. *Journal of the National Cancer Institute***53:** 661-674.

15 Care A, Silvani A, Meccia E, Mattia G, Stoppacciaro A, Parmiani G *et al* (1996). HOXB7 constitutively activates basic fibroblast growth factor in melanomas. *Mol Cell Biol***16:** 4842-4851.

16 Care A, Silvani A, Meccia E, Mattia G, Peschle C, Colombo MP (1998). Transduction of the SkBr3 breast carcinoma cell line with the HOXB7 gene induces bFGF expression, increases cell proliferation and reduces growth factor dependence. *Oncogene***16:** 3285-3289.

17 Chen H, Sukumar S (2003). Role of homeobox genes in normal mammary gland development and breast tumorigenesis. *Journal of mammary gland biology and neoplasia***8:** 159-175.

18 Chen H, Lee JS, Liang X, Zhang H, Zhu T, Zhang Z *et al* (2008). Hoxb7 inhibits transgenic HER-2/neu-induced mouse mammary tumor onset but promotes progression and lung metastasis. *Cancer Res***68:** 3637-3644.

19 Corso G, Figueiredo J, De Angelis SP, Corso F, Girardi A, Pereira J *et al* (2020). E-cadherin deregulation in breast cancer. *Journal of cellular and molecular medicine***24:** 5930-5936.

20 Dai X, Cheng H, Bai Z, Li J (2017). Breast Cancer Cell Line Classification and Its Relevance with Breast Tumor Subtyping. *J Cancer***8:** 3131-3141.

21 de Bessa Garcia SA, Pereira MC, Nagai MA (2010). Expression Pattern of the Pro-apoptotic Gene PAR-4 During the Morphogenesis of MCF-10A Human Mammary Epithelial Cells. *Cancer microenvironment : official journal of the International Cancer Microenvironment Society***4:** 33-38.

22 de Bessa Garcia SA, Araujo M, Pereira T, Mouta J, Freitas R (2020). HOX genes function in Breast Cancer development. *Biochim Biophys Acta Rev Cancer***1873:** 188358.

23 De Kumar B, Krumlauf R (2016). HOXs and lincRNAs: Two sides of the same coin. *Sci Adv***2:** e1501402.

24 Debnath J, Muthuswamy SK, Brugge JS (2003). Morphogenesis and oncogenesis of MCF-10A mammary epithelial acini grown in three-dimensional basement membrane cultures. *Methods***30:** 256-268.

25 Esposito E, Napolitano G, Pescatore A, Calculli G, Incoronato MR, Leonardi A *et al* (2016). COMMD7 as a novel NEMO interacting protein involved in the termination of NF-κB signaling. *Journal of cellular physiology***231:** 152-161.

26 Franken NA, Rodermond HM, Stap J, Haveman J, van Bree C (2006). Clonogenic assay of cells in vitro. *Nat Protoc***1:** 2315-2319.

27 Garcia SAdB, Araújo M, Freitas R (2020). Dataset of HOXB7, HOXB8 and HOXB9 expression profiles in cell lines representative of the breast cancer molecular subtypes Luminal a (MCF7), Luminal b (BT474), HER2+ (SKBR3) and triple-negative (MDA231, MDA468), compared to a model of normal cells (MCF10A). *Data in Brief***30:** 105572.

28 Gaunt SJ (2018). Hox cluster genes and collinearities throughout the tree of animal life. *Int J Dev Biol***62:** 673-683.

29 Heinonen H, Lepikhova T, Sahu B, Pehkonen H, Pihlajamaa P, Louhimo R *et al* (2015). Identification of several potential chromatin binding sites of HOXB7 and its downstream target genes in breast cancer. *Int J Cancer***137:** 2374-2383.

30 Hernández-Vargas H, Palacios J, Moreno-Bueno G (2007). Molecular profiling of docetaxel cytotoxicity in breast cancer cells: uncoupling of aberrant mitosis and apoptosis. *Oncogene***26:** 2902-2913.

31 Hur H, Lee JY, Yun HJ, Park BW, Kim MH (2014). Analysis of HOX gene expression patterns in human breast cancer. *Mol Biotechnol***56:** 64-71.

32 Jin K, Kong X, Shah T, Penet MF, Wildes F, Sgroi DC *et al* (2012). The HOXB7 protein renders breast cancer cells resistant to tamoxifen through activation of the EGFR pathway. *Proceedings of the National Academy of Sciences of the United States of America***109:** 2736-2741.

33 Jin K, Park S, Teo WW, Korangath P, Cho SS, Yoshida T *et al* (2015). HOXB7 Is an ERα Cofactor in the Activation of HER2 and Multiple ER Target Genes Leading to Endocrine Resistance. *Cancer discovery***5:** 944-959.

34 Kai K, Iwamoto T, Zhang D, Shen L, Takahashi Y, Rao A *et al* (2018). CSF-1/CSF-1R axis is associated with epithelial/mesenchymal hybrid phenotype in epithelial-like inflammatory breast cancer. *Scientific reports***8:** 9427.

35 Kamkar F, Xaymardan M, Asli NS (2016). Hox-Mediated Spatial and Temporal Coding of Stem Cells in Homeostasis and Neoplasia. *Stem cells and development***25:** 1282-1289.

36 Karamanou K, Franchi M, Vynios D, Brézillon S (2020). Epithelial-to-mesenchymal transition and invadopodia markers in breast cancer: Lumican a key regulator. *Seminars in cancer biology***62:** 125-133.

37 Kariri YA, Aleskandarany MA, Joseph C, Kurozumi S, Mohammed OJ, Toss MS *et al* (2020). Molecular Complexity of Lymphovascular Invasion: The Role of Cell Migration in Breast Cancer as a Prototype. *Pathobiology*.

38 Khramtsov AI, Khramtsova GF, Tretiakova M, Huo D, Olopade OI, Goss KH (2010). Wnt/beta-catenin pathway activation is enriched in basal-like breast cancers and predicts poor outcome. *The American journal of pathology***176:** 2911-2920.

39 Kraus LA, Samuel SK, Schmid SM, Dykes DJ, Waud WR, Bissery MC (2003). The mechanism of action of docetaxel (Taxotere®) in xenograft models is not limited to bcl-2 phosphorylation. *Investigational New Drugs***21:** 259-268.

40 Krumlauf R (2018). Hox genes, clusters and collinearity. *Int J Dev Biol***62:** 659-663.

41 Kumar P, Aggarwal R (2016). An overview of triple-negative breast cancer. *Archives of gynecology and obstetrics***293:** 247-269.

42 Lacazette E (2017). A laboratory practical illustrating the use of the ChIP-qPCR method in a robust model: Estrogen receptor alpha immunoprecipitation using Mcf-7 culture cells. *Biochemistry and Molecular Biology Education***45:** 152-160.

43 Lee GY, Kenny PA, Lee EH, Bissell MJ (2007). Three-dimensional culture models of normal and malignant breast epithelial cells. *Nat Methods***4:** 359-365.

44 Li G, Hu J, Hu G (2017). Biomarker Studies in Early Detection and Prognosis of Breast Cancer. In: Song E, Hu H (eds). *Translational Research in Breast Cancer: Biomarker Diagnosis, Targeted Therapies and Approaches to Precision Medicine*. Springer Singapore: Singapore. pp 27-39.

45 Li X, Yang J, Peng L, Sahin AA, Huo L, Ward KC *et al* (2017). Triple-negative breast cancer has worse overall survival and cause-specific survival than non-triple-negative breast cancer. *Breast cancer research and treatment***161:** 279-287.

46 Lin D, Kuang G, Wan J, Zhang X, Li H, Gong X *et al* (2017). Luteolin suppresses the metastasis of triple-negative breast cancer by reversing epithelial-to-mesenchymal transition via downregulation of β-

catenin expression. *Oncology reports***37:** 895-902.

47 Liu S, Jin K, Hui Y, Fu J, Jie C, Feng S *et al* (2015). HOXB7 promotes malignant progression by activating the TGFβ signaling pathway. *Cancer research***75:** 709-719.

48 Lyko F (2018). The DNA methyltransferase family: a versatile toolkit for epigenetic regulation. *Nature reviews Genetics***19:** 81-92.

49 Ma R, Zhang D, Hu P-C, Li Q, Lin C-Y (2015). HOXB7-S3 inhibits the proliferation and invasion of MCF-7 human breast cancer cells. *Mol Med Rep***12:** 4901-4908.

50 Milioli HH, Tishchenko I, Riveros C, Berretta R, Moscato P (2017). Basal-like breast cancer: molecular profiles, clinical features and survival outcomes. *BMC medical genomics***10:** 19.

51 Oliphant MUJ, Kong D, Zhou H, Lewis MT, Ford HL (2020). Two Sides of the Same Coin: The Role of Developmental pathways and pluripotency factors in normal mammary stem cells and breast cancer metastasis. *Journal of mammary gland biology and neoplasia***25:** 85-102.

52 Onitilo AA, Engel JM, Greenlee RT, Mukesh BN (2009). Breast cancer subtypes based on ER/PR and Her2 expression: comparison of clinicopathologic features and survival. *Clinical medicine & research***7:** 4-13.

53 Paço A, de Bessa Garcia SA, Freitas R (2020). Methylation in HOX Clusters and Its Applications in Cancer Therapy. *Cells***9**.

54 Prat A, Pineda E, Adamo B, Galván P, Fernández A, Gaba L *et al* (2015). Clinical implications of the intrinsic molecular subtypes of breast cancer. *Breast (Edinburgh, Scotland)***24 Suppl 2:** S26-35.

55 Roskoski R, Jr. (2014). The ErbB/HER family of protein-tyrosine kinases and cancer. *Pharmacological research***79:** 34-74.

56 Ross JM (1998). Chapter II. 1 - Cell-Extracellular Matrix Interactions. In: Patrick CW, Mikos AG, McIntire LV, Langer RS (eds). *Frontiers in Tissue Engineering*. Pergamon: Oxford. pp 15-27.

57 Sanchez-Herrero E (2013). Hox targets and cellular functions. *Scientifica (Cairo)***2013:** 738257.

58 Schmittgen TD, Livak KJ (2008). Analyzing real-time PCR data by the comparative CT method. *Nature Protocols***3:** 1101-1108.

59 Schneider CA, Rasband WS, Eliceiri KW (2012). NIH Image to ImageJ: 25 years of image analysis. *Nature Methods***9:** 671-675.

60 Shah N, Mohammad AS, Saralkar P, Sprowls SA, Vickers SD, John D *et al* (2018). Investigational chemotherapy and novel pharmacokinetic mechanisms for the treatment of breast cancer brain metastases. *Pharmacological research***132:** 47-68.

61 Subik K, Lee JF, Baxter L, Strzepek T, Costello D, Crowley P *et al* (2010). The Expression Patterns of ER, PR, HER2, CK5/6, EGFR, Ki-67 and AR by Immunohistochemical Analysis in Breast Cancer Cell Lines. *Breast Cancer (Auckl)***4:** 35-41.

62 Subramaniam D, Thombre R, Dhar A, Anant S (2014). DNA methyltransferases: a novel target for prevention and therapy. *Frontiers in oncology***4:** 80.

63 Takahashi K, Yamanaka S (2006). Induction of pluripotent stem cells from mouse embryonic and adult fibroblast cultures by defined factors. *Cell***126:** 663-676.

64 Tasdemir N, Bossart EA, Li Z, Zhu L, Sikora MJ, Levine KM *et al* (2018). Comprehensive Phenotypic Characterization of Human Invasive Lobular Carcinoma Cell Lines in 2D and 3D Cultures. *Cancer research***78:** 6209-6222.

65 Valenta T, Hausmann G, Basler K (2012). The many faces and functions of β-catenin. *The EMBO journal***31:** 2714-2736.

66 Waks AG, Winer EP (2019). Breast Cancer Treatment. *JAMA***321:** 316-316.

67 Wu X, Chen H, Parker B, Rubin E, Zhu T, Lee JS *et al* (2006). HOXB7, a homeodomain protein, is overexpressed in breast cancer and confers epithelial-mesenchymal transition. *Cancer research***66:** 9527-9534.

68 Xu J, Prosperi JR, Choudhury N, Olopade OI, Goss KH (2015). β-Catenin is required for the tumorigenic behavior of triple-negative breast cancer cells. *PLoS One***10:** e0117097.

69 You N, Li J, Gong Z, Huang X, Wang W, Wang L *et al* (2017). COMMD7 functions as molecular target in pancreatic ductal adenocarcinoma. *Molecular carcinogenesis***56:** 607-624.

70 You N, Li J, Huang X, Wu K, Tang Y, Wang L *et al* (2017). COMMD7 promotes hepatocellular carcinoma through regulating CXCL10. *Biomedicine & pharmacotherapy = Biomedecine & pharmacotherapie***88:** 653-657.

71 Zheng L, You N, Huang X, Gu H, Wu K, Mi N *et al* (2019). COMMD7 Regulates NF-κB Signaling Pathway in Hepatocellular Carcinoma Stem-like Cells. *Molecular therapy oncolytics***12:** 112-123.

72 Zugmaier G, Ennis BW, Deschauer B, Katz D, Knabbe C, Wilding G *et al* (1989). Transforming growth factors type beta 1 and beta 2 are equipotent growth inhibitors of human breast cancer cell lines. *Journal of cellular physiology***141:** 353-361.

Figures

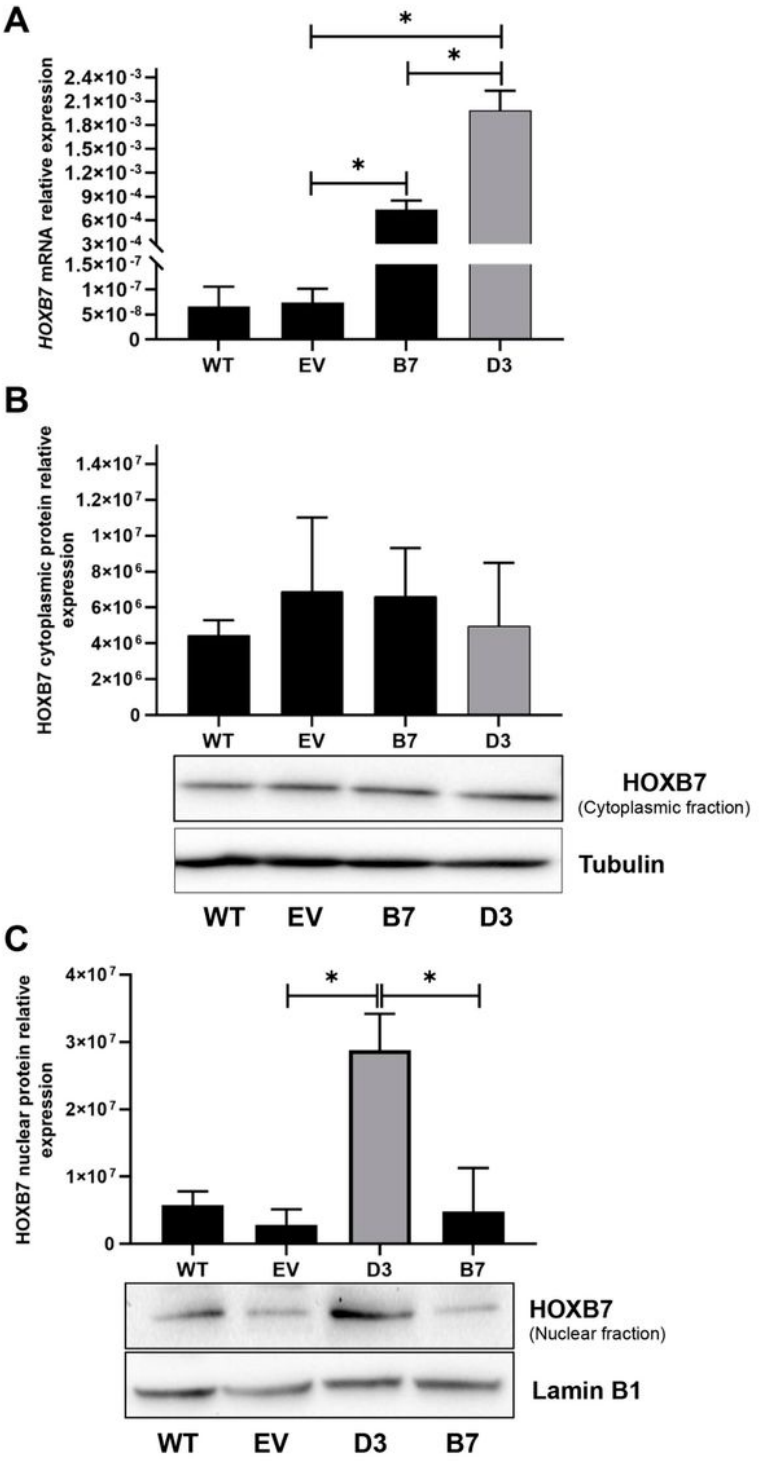

Figure 1

HOXB7 mRNA and protein expression characterization in MDA231 cells after transfection. A, HOXB7 mRNA expression in WT (wild-type cells), EV (empty-vector transfected cells), B7 (pool of cells transfected with HOXB7-expression vector), D3 (clone of cells transfected with HOXB7-expression vector). B, HOXB7 cytoplasmic protein expression in WT (wild type cells), EV (empty-vector transfected cells), B7 (pool of cells transfected with HOXB7-expression vector), D3 (clone of cells transfected with HOXB7-expression

vector). C, HOXB7 nuclear protein expression in WT (wild type cells), EV (empty-vector transfected cells), B7 (pool of cells transfected with HOXB7-expression vector), D3 (clone of cells transfected with HOXB7-expression vector). The bars represent the mean ±SD obtained in at least three independent experiments. *, Statistically significant differences, P≤0.05, obtained by Brown-Forsythe and Welch ANOVA tests (Multiple comparisons) with Games-Howell's correction.

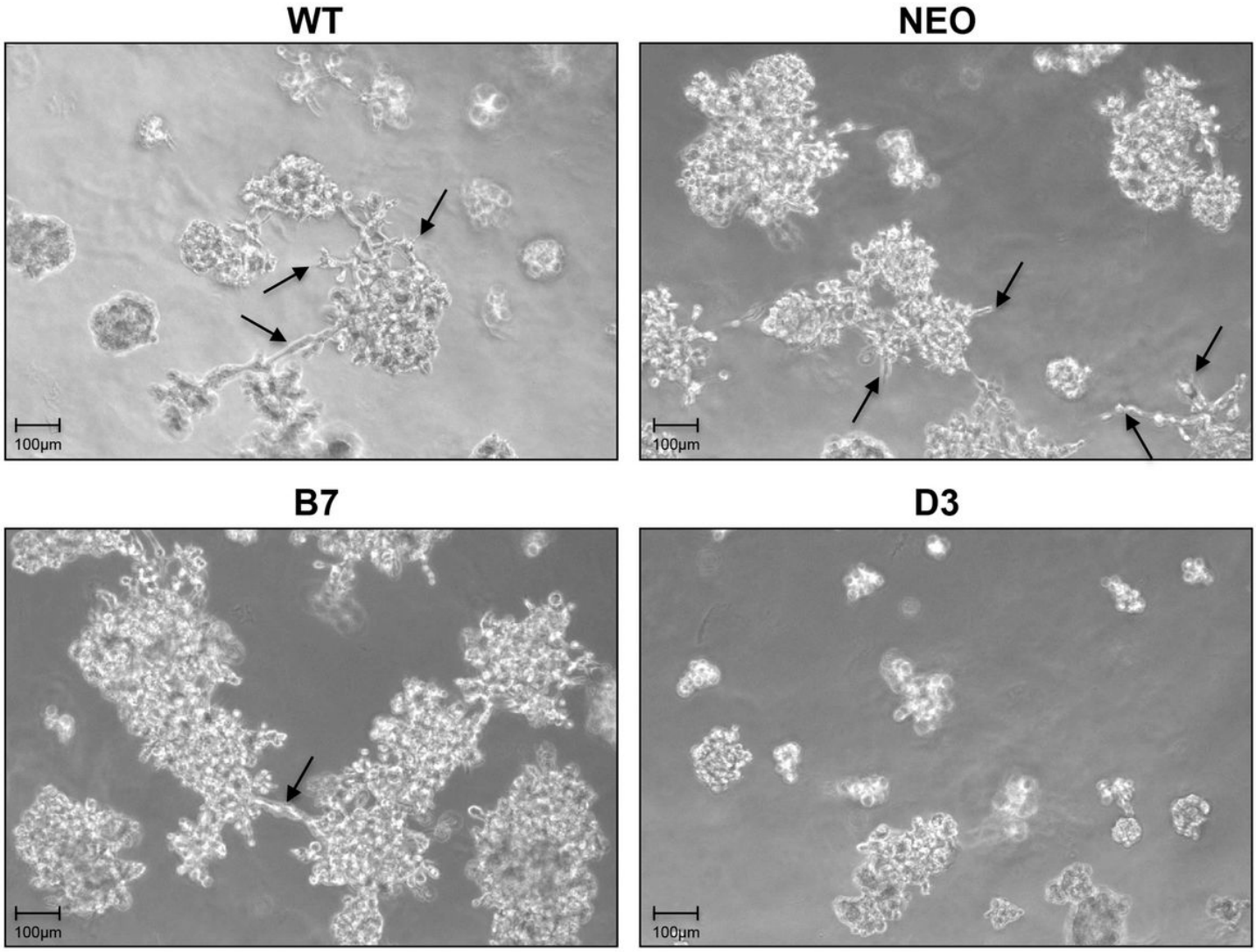

Figure 2

HOXB7 overexpression effect on MDA231 cells spheroids morphology in 3D cell culture. The cells were seeded in 8-well glass slides on-top in Matrigel® and after 8-days they were photographed in an inverted fluorescent microscope. The WT, EV and B7 cells show a similar pattern of 3D-growth with spread spheroids that form a number of protrusions. These patterns are clearly different from that observed in D3 cells, which grow in compact spheroids without protrusions formation.

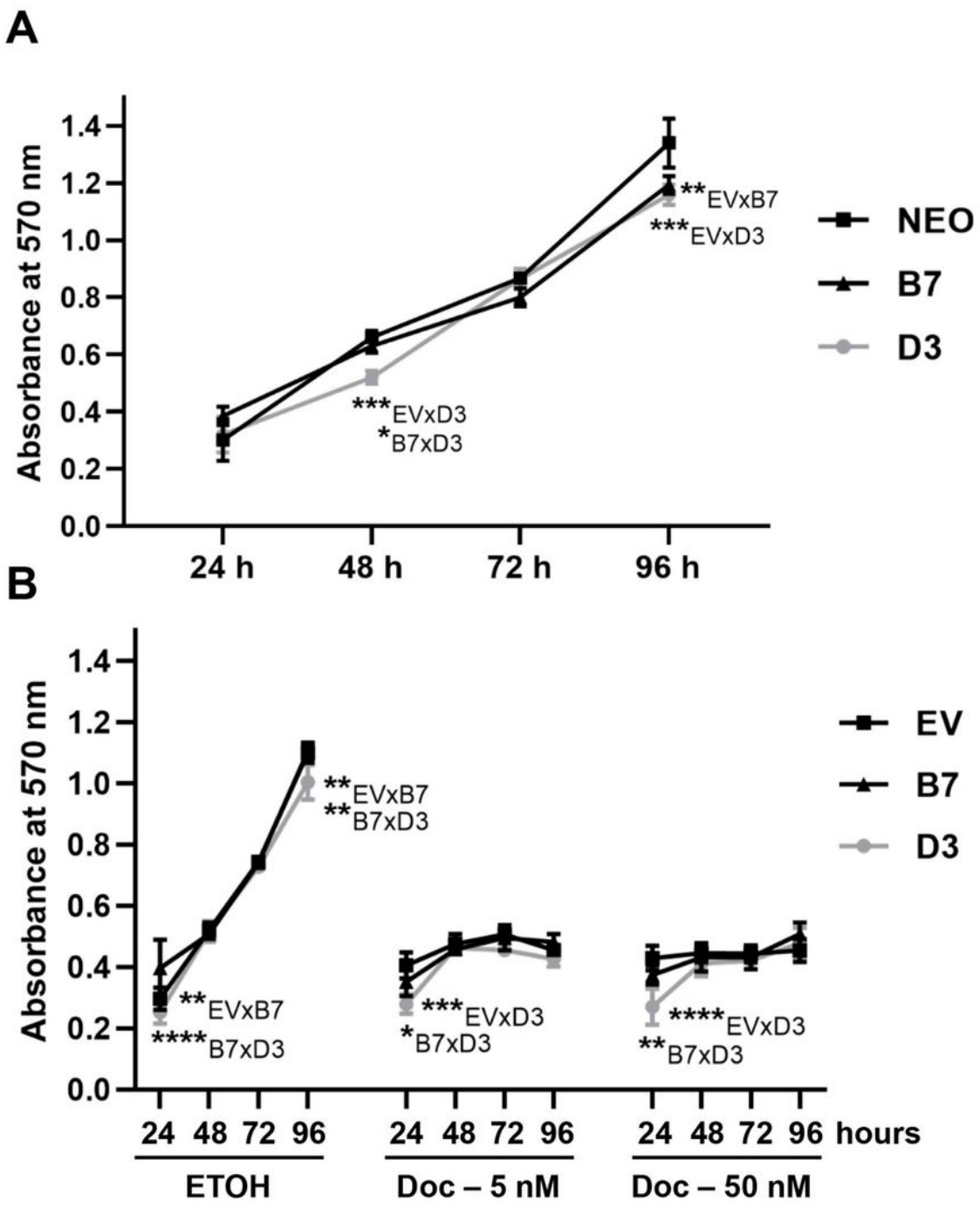

Figure 3

HOXB7 overexpression effect on viability and Docetaxel sensitivity of MDA231 cells. A, MTT cell-viability measure in EV, B7 and D3 cells in 24h, 48h, 72h and 96h post-plating. B, EV, B7 and D3 cell sensitivity to 5nM and 50nM Docetaxel treatment in 24h, 48h, 72h and 96h post-plating. The cells were kept in ETOH as a control of vehicle action. The graphs represent the mean ±SD obtained in at least three independent experiments. *, Statistically significant differences, P≤0.05, obtained through 2way ANOVA test (Multiple

comparisons) with Tukey's correction. In B, the P values for the time-point of 24h are: ETOH, EVxB7 (P=0.003) and B7xD3 (P=<0.0001); Docetaxel 5nM EVxD3 (P=0.0002) and B7xD3 (P=0.04); and Docetaxel 50nM EVxD3 (P<0.0001) and B7xD3 (P=0.0022).

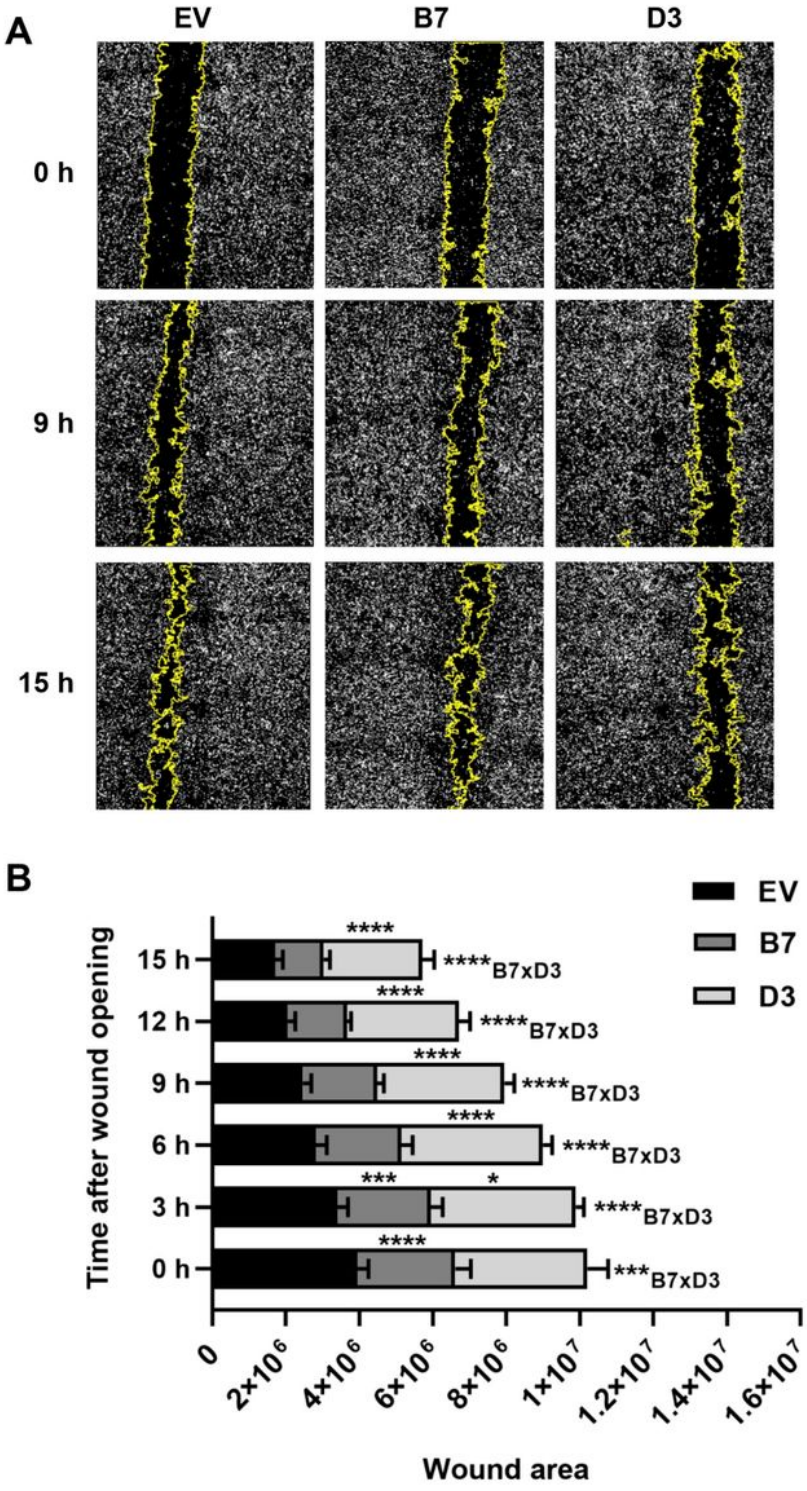

Figure 4

HOXB7 overexpression effect on MDA231 cells migration capacity. A, representative images of the wound healing assay in EV, B7 and D3 cells at 0h, 9h and 15h after the scratch wound. B, wound areas of the EV,

B7 and D3 cells along the time. The graph represents the mean ±SD obtained in at least three independent experiments. *, Statistically significant differences, P≤0.05, obtained through 2way ANOVA test (Multiple comparisons) with Tukey's correction. *, Represents the comparison between EV cells and the cells of the respective rectangle, when not specified.

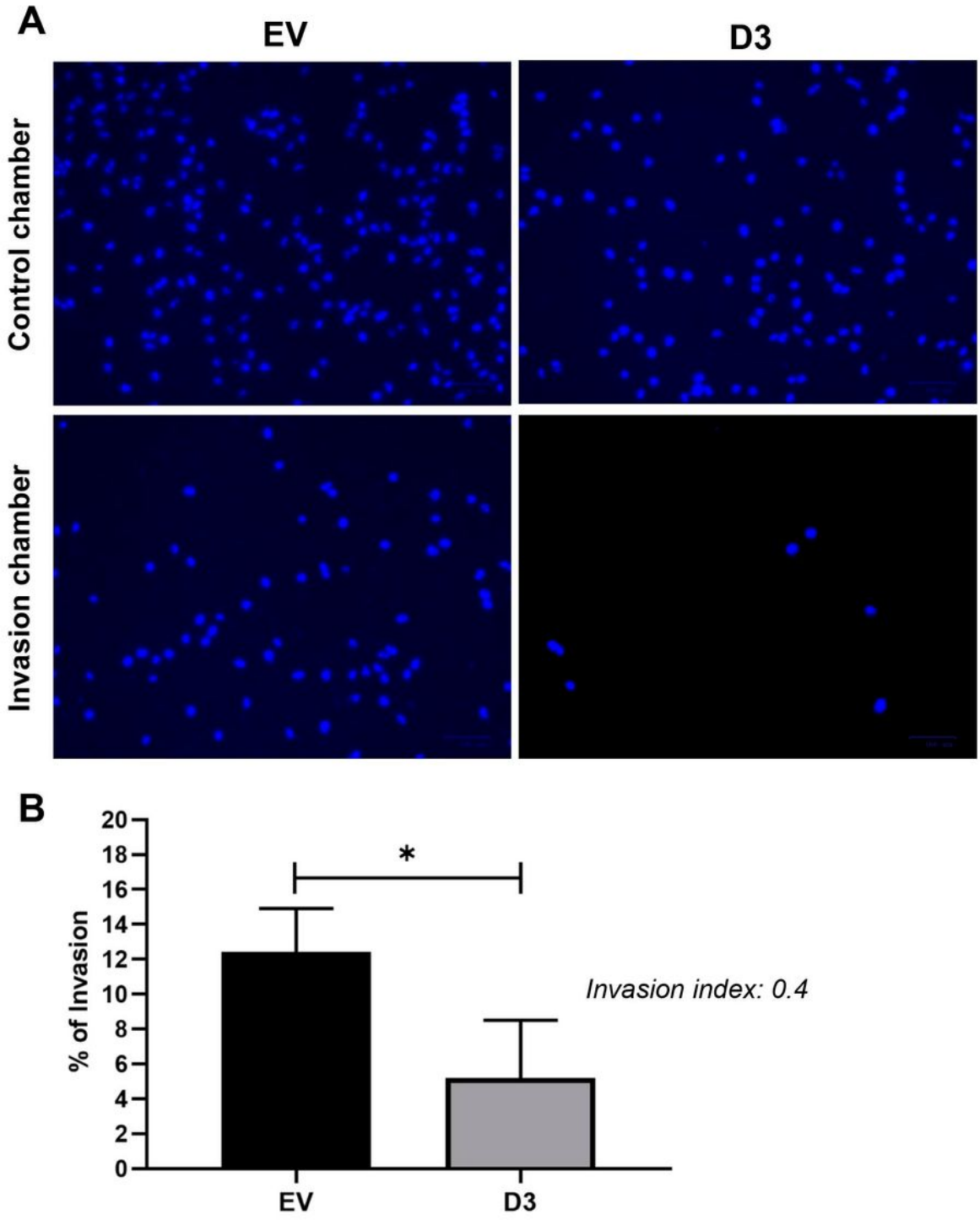

Figure 5

HOXB7 overexpression effect on MDA231 cells invasion capacity. A, representative images of the nuclei of the EV and D3 cells that invaded the Matrigel® layer of the invasion chamber and migrate through the control chambers. B, invasion percentage of EV and D3 cells with the respective invasion index. The graph represents the mean ±SD obtained in at least three independent experiments. * Statistically significant differences, P≤0.05, obtained by unpaired T test with Welch's correction.

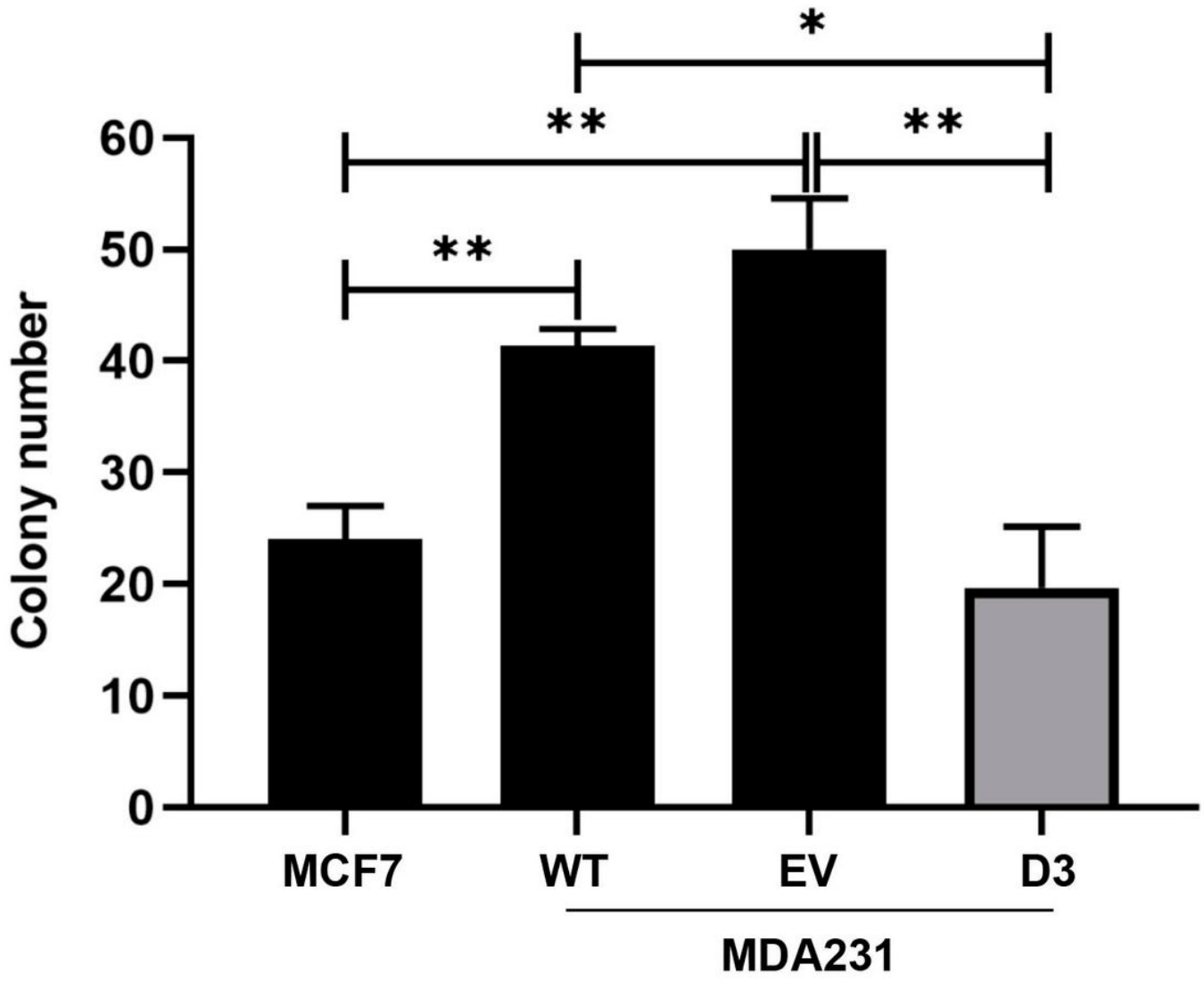

Figure 6

HOXB7 overexpression effect on MDA231 cells anchorage-independent colony formation efficiency. Number of colonies formed by MCF7 (Luminal A) and MDA231 (Triple-negative; WT, EV and D3). The graph represents the mean ±SD obtained in at least three independent experiments. *, Statistically significant differences, P≤0.05, obtained by Brown-Forsythe and Welch ANOVA tests (Multiple comparisons) with Games-Howell's correction.

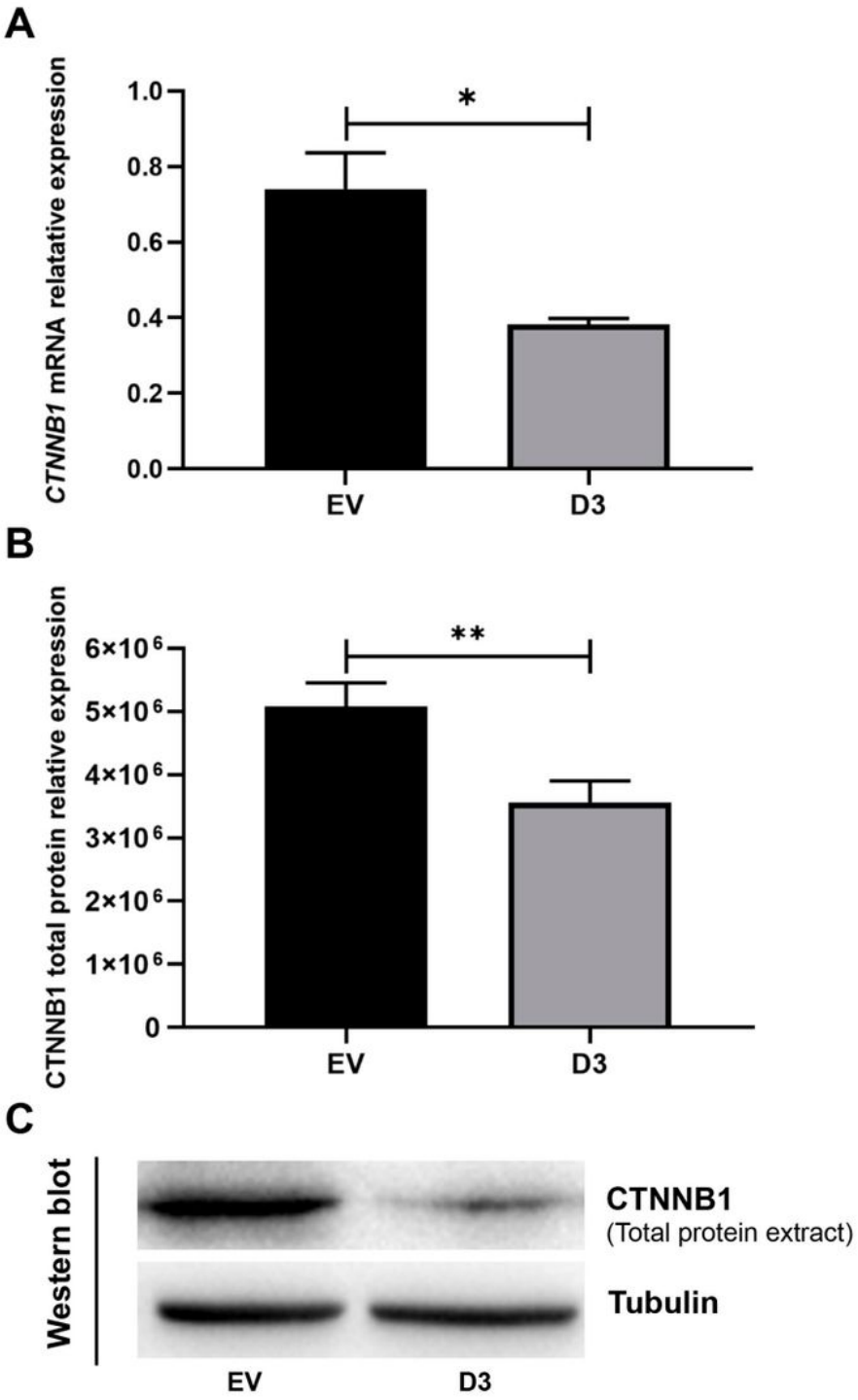

Figure 7

HOXB7 overexpression effect on CTNNB1 mRNA and protein expression in MDA231 cells. A, CTNNB1 mRNA relative expression in EV and D3 cells. B, CTNNB1 total protein relative expression EV and D3 cells. C, western blot representative of the CTNNB1 total protein analyses in EV and D3 cells being the expression of Tubulin the protein loading control. The bars represent the mean ±SD obtained in at least

three independent experiments. *, Statistically significant differences, P≤0.05, obtained by unpaired T test with Welch's correction.

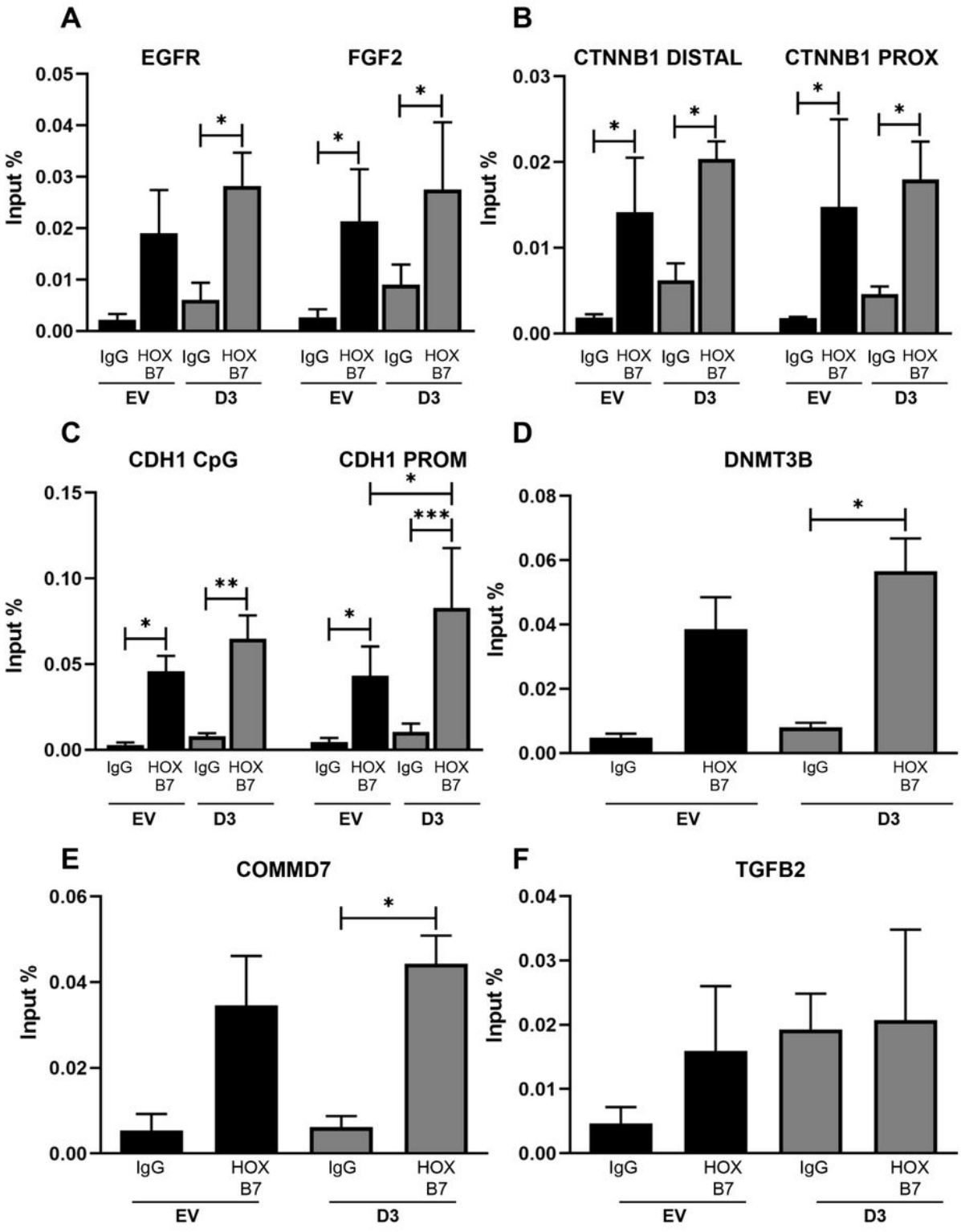

Figure 8

HOXB7 protein direct interaction with the promoter regions of EGFR (A), FGF2 (A), CTNNB1 (B), CDH1 (C), DNMT3B (D), TGFB2 (E) and COMMD7 (F). IgG, Immunoprecipitations with anti-IgG antibody (interaction negative control). HOXB7, Immunoprecipitations with anti-HOXB7 antibody. The bars represent the mean

±SD obtained in at least three independent experiments. *, Statistically significant differences, P≤0.05, obtained by 2way ANOVA test (Multiple comparisons) with Bonferroni's correction (EGFR, FGF2, CTNNB1 DISTAL, CTNNB1 PROX, CDH1 CpG and CDH1 PROM) or by Brown-Forsythe and Welch ANOVA tests (Multiple comparisons) with Games-Howell's correction (DNMT3B, TGFB2 and COMMD7). The calculated P values were: EGFR (IgG_D3xD3=0.01), FGF2 (IgG_EVxEV=0.035, IgG_D3xD3=0.036), CTNNB1 (DISTAL: IgG_EVxEV=0.032, IgG_D3xD3=0.011. PROX: IgG_EVxEV=0.022, IgG_D3xD3=0.017), CDH1 (CpG: IgG_EVxEV=0.018, IgG_D3xD3=0.002. PROM: IgG_EVxEV=0.034, IgG_D3xD3=0.0001, EVxD3=0.031), DNMT3B (IgG_D3xD3=0.033) and COMMD7 (IgG_D3xD3=0.013).

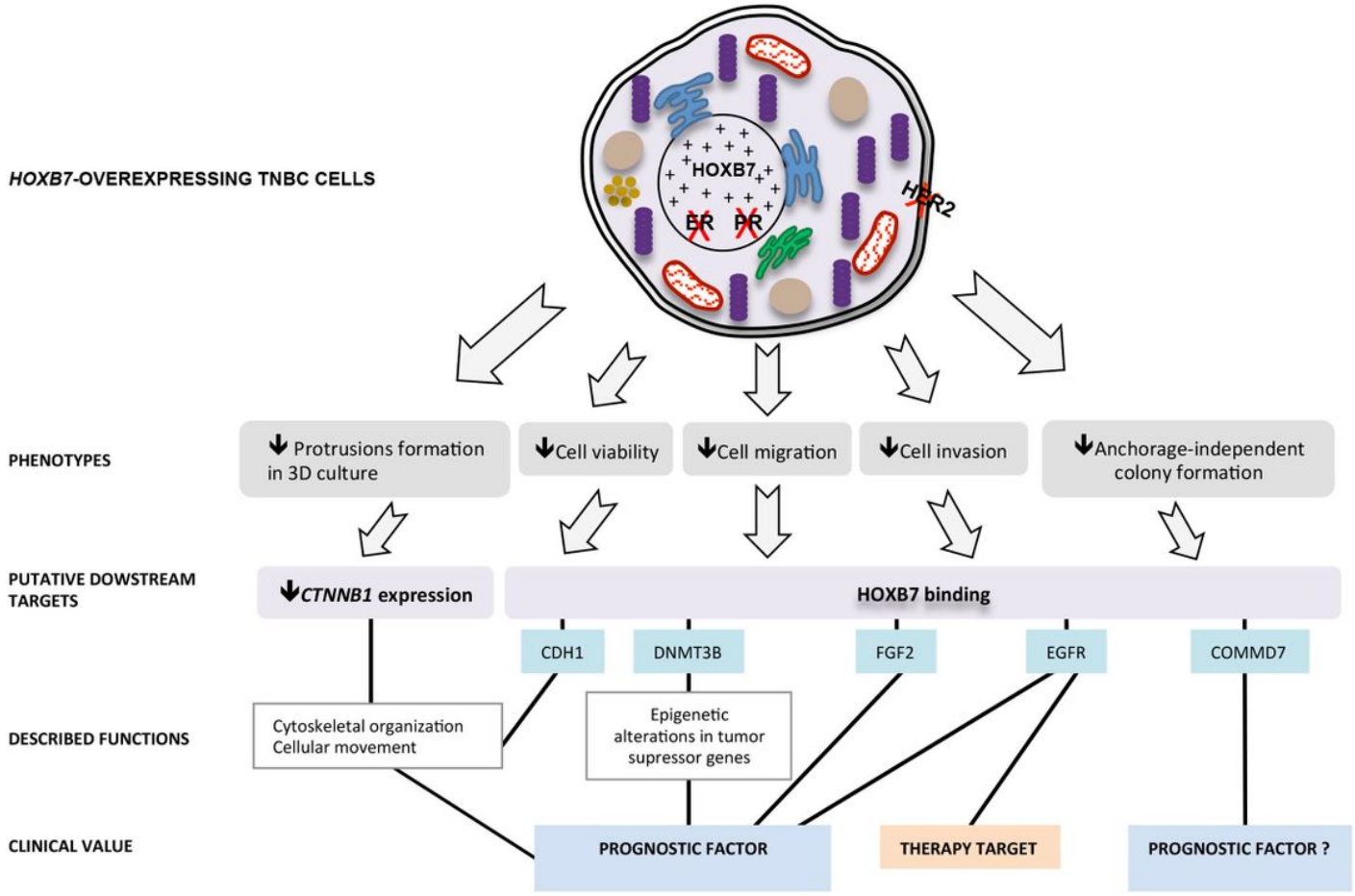

Figure 9

Summary of the HOXB7 nuclear overexpression effects in the TNBC cell line MDA-MB-231. The HOXB7 nuclear overexpression leads the MDA-MB-231 cells to a less aggressive phenotype represented by a more organized spheroid formation in 3D culture and reduced cell viability, migration, invasion and anchorage-independent colony formation. The observed phenotypes could be related to changes in CTNNB1 expression and to HOXB7 binding to genes with important roles in breast cancer progression. Exception made to COMMD7 whose function in cancer is still little studied.

Supplementary Files

This is a list of supplementary files associated with this preprint. Click to download.

- SupplementaryData.pdf